



Published in final edited form as:

Exp Brain Res. 2000 February ; 130(3): 277–297.

Afferent diversity and the organization of central vestibular pathways

Jay M. Goldberg

Department of Pharmacological and Physiological Sciences, 947 E. 58th St., Chicago, IL 60637, USA

Abstract

This review considers whether the vestibular system includes separate populations of sensory axons innervating individual organs and giving rise to distinct central pathways. There is a variability in the discharge properties of afferents supplying each organ. Discharge regularity provides a marker for this diversity since fibers which differ in this way also differ in many other properties. Postspike recovery of excitability determines the discharge regularity of an afferent and its sensitivity to depolarizing inputs. Sensitivity is small in regularly discharging afferents and large in irregularly discharging afferents. The enhanced sensitivity of irregular fibers explains their larger responses to sensory inputs, to efferent activation, and to externally applied galvanic currents, but not their distinctive response dynamics. Morphophysiological studies show that regular and irregular afferents innervate overlapping regions of the vestibular nuclei. Intracellular recordings of EPSPs reveal that some secondary vestibular neurons receive a restricted input from regular or irregular afferents, but that most such neurons receive a mixed input from both kinds of afferents. Anodal currents delivered to the labyrinth can result in a selective and reversible silencing of irregular afferents. Such a functional ablation can provide estimates of the relative contributions of regular and irregular inputs to a central neuron's discharge. From such estimates it is concluded that secondary neurons need not resemble their afferent inputs in discharge regularity or response dynamics. Several suggestions are made as to the potentially distinctive contributions made by regular and irregular afferents: (1) Reflecting their response dynamics, regular and irregular afferents could compensate for differences in the dynamic loads of various reflexes or of individual reflexes in different parts of their frequency range; (2) The gating of irregular inputs to secondary VOR neurons could modify the operation of reflexes under varying behavioral circumstances; (3) Two-dimensional sensitivity can arise from the convergence onto secondary neurons of otolith inputs differing in their directional properties and response dynamics; (4) Calyx afferents have relatively low gains when compared with irregular dimorphic afferents. This could serve to expand the stimulus range over which the response of calyx afferents remains linear, while at the same time preserving the other features peculiar to irregular afferents. Among those features are phasic response dynamics and large responses to efferent activation; (5) Because of the convergence of several afferents onto each secondary neuron, information transmission to the latter depends on the gain of individual afferents, but not on their discharge regularity.

Keywords

Vestibular nerve; Central vestibular pathways; Discharge regularity; Sensory processing; Information theory

Introduction

Both the somatosensory (Darian Smith 1984; Mountcastle 1984; Dykes et al. 1988; Johnson and Hsiao 1992) and visual pathways (Shapley 1990; Schiller and Logothetis 1990; Merigan and Maunsell 1993) can be viewed as being composed of several parallel channels. In both systems, sensory axons differ in their peripheral terminations, discharge properties, central projections, and functional contributions to discriminative behavior. Moreover, neurons at higher levels of the system resemble one or another class of sensory axon. A somewhat different arrangement occurs in the auditory system. In the cochlear nuclei, there are several populations of relay cells that differ in their discharge properties and projections to higher auditory centers (Aitkin et al. 1984; Hackney 1987; Palmer 1987). The differences in discharge properties may reflect the intrinsic physiology of the relay cells and their connections with the same and other parts of cochlear nuclei (Oertel 1991; Young et al. 1992; Trussell 1997, 1999) as much as or more than their connections with distinctive populations of cochlear-nerve fibers (Liberman 1982, 1991, 1993).

In the somatosensory and visual systems, afferent diversity is reflected in the organization of central pathways. The same is true of the vestibular system, especially when the pathways arising from separate organs are considered. There is ample evidence that parallel reflex pathways interconnect the three cristae and the two maculae with various motoneuron pools (see, for example, Cohen et al. 1964; Wilson and Maeda 1974; Ito et al. 1977; Peterson et al. 1992; Graf et al. 1993; Uchino et al. 1996; Sato et al. 1996, 1997). In most instances, the pathways match the directional properties of afferents with the pulling directions of muscles so that reflex movements compensate for passive head movements. A second kind of diversity is provided by the central connections of secondary neurons contributing to vestibuloocular (VOR) pathways. Only some of these neurons receive a monosynaptic inhibitory input from the cerebellar flocculus (Ito et al. 1977; Lisberger et al. 1994a). So-called flocculus-target (FTN) neurons and non-FTN neurons differ in their oculomotor and vestibular signals (Scudder and Fuchs 1992; Lisberger et al. 1994a; Cullen and McCrea 1993; Cullen et al. 1993) as well as in their functional roles in the operation and adaptive plasticity of the VOR (Lisberger et al. 1994a, 1994b; McConville and Tomlinson 1996; Chen-Huang and McCrea 1999a, 1999b).

This review will emphasize still another kind of diversity: that reflected in differences in the discharge properties of afferents innervating individual vestibular organs. The peripheral mechanisms responsible for such diversity will be reviewed because of their intrinsic importance, because they provide clues as to the distinctive functions of the various afferents groups, and because they form the basis for many of the methods used to delineate the contributions of the various groups to central pathways. In an attempt to understand the potential functions of this kind of afferent diversity, its impact on the organization of central vestibular pathways and on the encoding of sensory information will then be considered. Some of these topics have also been reviewed by Peterson (1998).

Peripheral mechanisms

Discharge regularity and other discharge properties

Discharge properties of vestibular-nerve fibers have been described in several mammals (Goldberg and Fernández 1971a, 1971b; Fernández and Goldberg 1971, 1976a, 1976b; Schneider and Anderson 1976; Baird et al. 1988; Goldberg et al. 1990a; Lysakowski et al. 1995) and in selected lower vertebrates, including the toadfish (Boyle and Highstein 1990a), frog (Honrubia et al. 1989; Myers and Lewis 1990), and turtle (Brichta and Goldberg 1996, 2000a). In most of these species, it has proved useful to distinguish afferents as having a regular or an irregular spacing of action potentials (Fig. 1). Interest in this discharge

property stems in part from the fact that fibers first classified as regularly or irregularly discharging differ in several other respects as well. Table 1 summarizes some of the differences for mammalian afferents, including those innervating the cristae and the maculae. In most respects, similar differences in axon diameter, response dynamics, and vestibular sensitivity are seen in lower vertebrates (for review, Goldberg and Brichta 1998). In all species studied, irregular afferents have much larger responses to electrical activation of efferent pathways than do regular afferents; this is so even though the efferent action on comparable groups of afferents can be excitatory in some species and inhibitory in others (Goldberg and Fernández 1980; Boyle and Highstein 1990b; Sugai et al. 1991; McCue and Guinan 1994; Brichta and Goldberg 1996, 2000b).

Discharge regularity is characteristic of each afferent. This can be seen in Fig. 2A, which plots the standard deviation (SD) of intervals versus the mean interval ($\bar{\tau}$) for three afferents. For each afferent, points obtained during the background discharge and during excitatory and inhibitory rotations fall along a single curve. Furthermore, the points for the three units remain separate with changes in mean interval or stimulus conditions. A quantitative measure of discharge regularity is provided by the coefficient of variation (cv), the ratio of SD to $\bar{\tau}$. The cv of an individual afferent varies with $\bar{\tau}$ (Fig. 2B, points). To obtain a measure independent of such variations, empirical formulas (Figs. 2B and 3A, curves) have been developed to determine for each unit its cv^* , the cv at a standard mean interval ($\bar{\tau}^*$).

For mammals, where the background $\bar{\tau}$ is typically 10–20 ms, $\bar{\tau}^*$ was set to 15 ms (Goldberg et al. 1984; Baird et al. 1988); in turtles, with their lower background rates, $\bar{\tau}^*$ was set to 50 ms (Brichta and Goldberg 1996, 2000a). cv^* varies 30-fold in mammals, from 0.02 to 0.6 (Fig. 3). The distribution of cv^* 's in mammals, while it has peaks centered at 0.03 and 0.3, is continuous so a division of the afferents into “regular” and “irregular” classes may be viewed as a rhetorical convenience. The range of cv^* 's in turtles (and probably in other non-mammalian species) is smaller (0.10–1.0). That the cv^* seldom falls below 0.1 can be partly explained by the lower rates found in these animals combined with a tendency for the cv^* to grow as $\bar{\tau}$ increases. From the normalization curves for mammals (Figs. 2B, 3A), a cv^* of 0.1 at $\bar{\tau}^*=50$ ms is equivalent to a cv^* of 0.0375 at $\bar{\tau}^*=15$ ms. At the same time, it is unlikely that the entire difference in cv^* 's can be explained by a rate difference. The smallest cv^* seen in mammals is near 0.025, which would correspond to a cv^* of 0.070 at $\bar{\tau}^*=50$ ms. Since the cv^* in turtles does not reach such a low value at $\bar{\tau}^*=50$ ms, it would appear that discharge is never as regular in turtles as it is in the most regular mammalian afferents.

There is a broad, continuous distribution of normalized cv's in vestibular-nerve axons (Fig. 3B). This is an unusual, possibly unique feature in a sensory system. As can be seen in Table 2, most retinal ganglion cells have a modestly irregular discharge (Troy and Robson 1992; Troy and Lee 1994), whereas cochlear afferents have a discharge that is especially irregular (Li and Young 1993; E. D. Young, personal communication). Isolated muscle-spindle afferents have a discharge that is particularly regular in secondary receptors; under fusimotor influence, discharge becomes less regular (Matthews and Stein 1969). Among slowly adapting cutaneous touch receptors, SA-I units are irregular, while SA-II receptors are regular (Iggo and Muir 1969). Of the several sensory systems included in the table, only the SA receptors show a range of cv's approaching that seen in the vestibular periphery. Even the SA fibers differ from vestibular afferents in falling into two distinct classes based on their discharge regularity and other properties.

Cellular mechanisms of discharge regularity

Which of the differences listed in Table 1 is causally related to discharge regularity? To answer this question requires an understanding of the cellular mechanisms determining the

spacing of action potentials. Intra-axonal recordings from vestibular-nerve axons suggest that the timing of spikes is determined by an afterhyperpolarization (AHP) following each spike (Highstein and Politoff 1978). AHPs play a similar role in other repetitively discharging neurons (Barrett and Barrett 1976; Connor 1978). The mechanisms determining discharge regularity in vestibular afferents were clarified by studying the effects on unitary discharge of externally applied galvanic currents, which were shown to modify discharge by acting on the spike encoder in the axon terminal (Goldberg et al. 1984). There were two key observations: (1) postspike recovery of excitability, as measured with short shocks placed at various times following naturally occurring action potentials, is fast in irregular fibers and slow in regular fibers (Fig. 4A); (2) sensitivity to galvanic currents (β^*) is related to discharge regularity: the larger the cv^* of a unit, the greater is its β^* (Fig. 4B).

To explain these results, a stochastic version of Kernell's (1968) AHP model of repetitive discharge was developed (Smith and Goldberg 1986; Fig. 5). In the model, each spike triggers a voltage-insensitive K^+ conductance (g_K), which sums with the conductance left over from previous spikes and declines exponentially with post-spike time. In both its voltage insensitivity and its summation across spikes, the conductance resembles the calcium-activated K^+ conductance responsible for AHPs in motoneurons (Barrett and Barrett 1976; Hille 1993). The only source of postsynaptic voltage fluctuations and, hence, of interspike variability is assumed to be synaptic noise, more specifically, the shot noise produced by randomly timed neurotransmitter quanta (Furukawa et al. 1978; Rossi et al. 1994); membrane noise, which is typically much smaller than synaptic noise (Verveen and De-Felice 1974), is ignored. To account for the relation between β^* and cv^* required that afferents differ in both their g_K 's and quantal amplitudes (A). In the model, irregular neurons have smaller, more rapidly decaying g_K 's and larger A 's than do regular neurons. All of the variation in β^* and most of that in cv^* are attributed to differences in g_K .

The model predicts that the sensitivities to synaptic and external currents parallel one another. In particular, irregular afferents should have an enhanced sensitivity to both kinds of inputs. Of the several differences listed in Table 1, irregular fibers would be expected to have a greater sensitivity to sensory inputs, to efferent activation, and to externally applied galvanic currents. Fiber size, while it is known to affect electrical excitability, had a much smaller effect on galvanic sensitivity than did discharge regularity (Goldberg et al. 1984). Of the various physiological differences between regular and irregular fibers, only the relation between discharge regularity and response dynamics is not predicted by the model. To investigate the etiology of this relation, afferent responses to sinusoidal head rotations and sinusoidally modulated electric currents were compared. While the response dynamics characterizing the responses to head rotations differed for regular and irregular units, that characterizing galvanic stimulation did not (Goldberg et al. 1982; Ezure et al. 1983). Results are consistent with the conclusion that differences in response dynamics arise at an earlier stage of hair-cell transduction than do differences in discharge regularity (Highstein et al. 1996). In addition, the conclusion illustrates that two discharge properties – in this case discharge regularity and response dynamics – can be highly correlated without being causally related.

Discharge regularity, innervation patterns, and locations of terminals in the neuroepithelium

Based on the morphology of their peripheral terminal arbors, three kinds of afferents can be recognized in mammalian vestibular organs (Fig. 6) (Fernández et al. 1988, 1990, 1995). Calyx fibers provide calyx endings to 1–3 neighboring type-I hair cells (Fig. 6A, B). Bouton fibers give rise to several (15–100) bouton endings contacting type-II hair cells over distances of 25–75 μm (Fig. 6H). Dimorphic fibers provide a mixed innervation of 1–4 calyx endings to type-I hair cells and 1–50 bouton endings to type-II hair cells (Fig. 6C–G).

The three kinds of fibers have different distributions within the crista (Fig. 6 right). Calyx units are largely confined to a central zone and bouton units to a concentrically arranged peripheral zone, while dimorphic units are found throughout the neuroepithelium (Fernández et al. 1988, 1995). Similarly, in the chinchilla utricular macula, dimorphic units are distributed throughout the organ, including the striola, juxtastriola, and peripheral extrastriola; calyx units are restricted to the striola and the very few bouton units are found in the peripheral extrastriola (Fernández et al. 1990).

In anamniotes (fish, amphibians), the crista contains only type-II hair cells innervated by non-calyceal fibers (Wersäll and Bagger-Sjöbäck 1974; Lysakowski 1996). In addition to boutons, some of the endings are described as claw-shaped (Honrubia et al. 1989) or club-shaped (Boyle et al. 1991). The results of afferent-labeling studies suggest that the anamniote crista, rather than being concentrically organized as in mammals, consists of a single, longitudinally organized zone (Honrubia et al. 1989; Myers and Lewis 1990; Boyle et al. 1991). Afferents innervating the neuroepithelium near the planum have thinner axons and simpler arbors than those supplying the isthmus region in the center of the crista. The turtle cristae consist of one or two hemicristae (Jørgensen 1974; Brichta and Peterson 1994). Each hemicrista has a peripheral zone surrounding a central zone. The peripheral zone is longitudinally organized, contains only type-II hair cells, and is similar in innervation to the entire half crista of anamniotes. Type-I and fewer type-II hair cells are found in the central zone and are innervated by a mixture of calyx, dimorphic, and bouton fibers (Brichta and Peterson 1994).

Discharge regularity is largely determined by the characteristics of an AHP, which, in turn, should reflect the afferent terminal's ionic currents, rather than its branching patterns or the types and number of hair cells it innervates. Branching patterns, as such, might affect discharge regularity because the electrotonic distance between afferent synapses and the encoder could influence quantal size and, hence, synaptic noise. Compartmental cable calculations (J.M. Goldberg and C. Fernández, unpublished results), when combined with Smith and Goldberg's (1986) stochastic model, suggest that electrotonic distance would have only a small effect on discharge regularity.

Morphophysiological results are consistent with the conclusion that branching patterns are not a major determinant of discharge regularity. In mammals, calyx and dimorphic units in the central (striolar) zone are both irregularly discharging, whereas bouton and dimorphic units in the peripheral (peripheral extrastricular) zone are regularly discharging; in a similar vein, dimorphic units innervating different parts of the neuroepithelium differ in cv^* , even when the units have similar branching patterns (Baird et al. 1988; Goldberg et al. 1990b). Results from lower vertebrates reinforce the conclusion. In the cristae of anamniotes (Honrubia et al. 1989; Boyle et al. 1991) and in the peripheral zone of the turtle crista (Brichta and Goldberg 1996, 2000a), regular and irregular units are found near the planum and isthmus, respectively. This would be hard to explain by branching patterns, which are simpler near the planum. In addition, calyx and dimorphic units in the turtle central zone are as irregularly discharging as are the bouton units found in the isthmus.

These findings imply that discharge regularity is correlated with neuroepithelial location, more so than it is with branching patterns or kinds of endings. The simplest interpretation is that the ionic currents determining interspike trajectories (Fig. 5) vary with place in the neuroepithelium.

Discharge regularity and gain to natural stimulation

For reasons that are not well understood, electric currents delivered by way of the perilymphatic space influence discharge by acting on the spike encoder in the axon terminal,

rather than on hair cells or the parent axon (Goldberg et al. 1984). Because of this, galvanic sensitivity (β^*) can be thought of as a measure of encoder gain, and the ratio between the gain to natural stimulation and β^* can be viewed as a measure of the synaptic input delivered to the encoder. This idea can be illustrated with data from the chinchilla crista (Baird et al. 1988; Goldberg et al. 1990c).

Figure 7 plots 2-Hz sinusoidal gains ($g_{2\text{ Hz}}$) and phases ($\phi_{2\text{ Hz}}$) re head velocity versus cv^* for both intra-axonally labeled and extracellularly recorded afferents. While there is a single, semilogarithmic relation between $\phi_{2\text{ Hz}}$ and cv^* (Fig. 7B), two groups are evident in the corresponding relation for $g_{2\text{ Hz}}$ (Fig. 7A). For one group, which includes all dimorphic and the one bouton unit recovered in the study, $g_{2\text{ Hz}}$ increases almost linearly with cv^* . Two factors contribute to the regression. The smaller of the two is a dynamic effect, the high-frequency gain enhancement associated with the phase lead seen at 2 Hz. To eliminate the effect, we can use gains at 0.2 Hz, where inter-unit differences in phase and, by inference, in response dynamics are minimal. When this is done (Fig. 7C), it is found that the relation between $g_{0.2\text{ Hz}}$ and cv^* for the first group gives a power-law with an exponent that is statistically indistinguishable from the exponent for the β^* versus cv^* relation (Fig. 4B). As suggested in the preceding paragraph, the synaptic input to the encoder can be estimated from the ratio, $g_{0.2\text{ Hz}}/\beta^*$ (Fig. 7D). Synaptic input is nearly constant for the first group. The second group is made up of calyx units. They are the most irregularly discharging units in the sample, have the largest 2-Hz phase leads, and have a mean synaptic input five times lower than that of the first group.

The synaptic inputs calculated for the two groups can be used to estimate the synaptic weights contributed by each calyx (w_C) and bouton (w_B) ending. The $w_C:w_B$ ratio is 3:1 (Baird et al. 1988). This is a surprisingly low value, considering that each calyx ending is contacted by an average of 15–20 \times the number of afferent (ribbon) synapses contacting each bouton ending (Lysakowski and Goldberg 1997). A possible explanation for the relatively small synaptic weights of calyx endings is provided by studies of the electrophysiology of type-I hair cells. As first described by Correia and Lang (1990), type-I hair cells have a distinctive outwardly rectifying K^+ current (Rennie and Correia 1994; Rüschi and Eatock 1996a, 1996b; Brichta and Goldberg 1998; Brichta et al. 1998), which gives them a low input impedance and, hence, a small voltage response to transducer currents. Regardless of its etiology, the low gains of calyx units should allow them to encode over a larger stimulus range than can irregular dimorphic units.

Central mechanisms

Central terminations of vestibular-nerve afferents

Labeling of individual axons—Sato et al. (1989; Sato and Sasaki 1993) labeled the central processes of individual cat horizontal-canal fibers characterized electrophysiologically by their discharge regularity (Fig. 8). Few of the labeled afferents terminate in the lateral vestibular nucleus (LVN) and most of these are irregular. Individual regular (Fig. 8A, right) and irregular fibers (Fig. 8B, right) innervate overlapping regions of the superior (SVN), medial (MVN), and descending or inferior (IVN) vestibular nuclei. Although they project to the same territories, the two kinds of fibers differ in their modes of termination. Irregular, as compared with regular, fibers have fewer, thicker, and longer preterminal collaterals, with each collateral containing fewer, but larger boutons. On average, there are 2–3 \times as many boutons on regular fibers. The proximal innervation of neurons with the largest cell bodies is derived almost exclusively from irregular fibers (cf. Fig. 8A, left with Fig. 8B, left). Smaller neurons may receive their proximal innervation from regular or irregular afferents. It is unclear whether there is a relation between cell size and the afferent innervation of distal dendrites.

A similar analysis has been done in the toadfish (Mensing et al. 1997). The authors classified horizontal-canal afferents by their gains and phases. As was the situation in the cat, the central projections of the various kinds of afferents overlapped, but differed in their branching patterns. Huwe and Peterson (1995), by labeling individual posterior-crista axons in turtles, have found that the descending branches of thick fibers preferentially innervate rostral parts of the vestibular nuclei.

Electrophysiological studies—Since regular and irregular afferents innervate overlapping territories in the mammalian vestibular nuclei, it is unclear whether the two kinds of afferents supply the same or different secondary neurons. To ascertain this in the squirrel monkey, use was made of the fact that irregular afferents are recruited by brief shocks at lower thresholds than are regular afferents (Goldberg et al. 1984, 1987). Monosynaptic EPSPs were recorded intracellularly as a test shock delivered to the ipsilateral vestibular nerve (V_i) was increased in amplitude. The test shock was preceded by a fixed, suprathreshold conditioning shock to synchronize the activity of all vestibular-nerve fibers.

Neurons whose V_i EPSPs reach maximum at low shock strengths are thought to receive a predominantly irregular input (Fig. 9A), while those whose V_i EPSPs have high shock thresholds are interpreted as receiving a mostly regular input (Fig. 9D). Most secondary neurons appear to receive a mixed input since they have low-threshold V_i EPSPs that continue to grow as shock strength is raised to high levels (Fig. 9B, C). At the same time, neurons identified by antidromic techniques or intrasomatic labeling as projecting into oculomotor (VO), cervical spinal (VC), or both oculomotor and cervical spinal pathways (VOC) tend to have different mixtures of regular and irregular afferent inputs (Highstein et al. 1987; Boyle et al. 1992). VO neurons commonly receive a mixed input. VC neurons, particularly those antidromically activated from the upper, but not the lower cervical cord, receive a predominantly irregular input, while the input to VOC neurons is predominantly regular.

Similar electrophysiological methods have now been employed in the isolated brain of the frog (Straka and Dieringer 1996; Straka et al. 1997). However, here the afferents, because they were disconnected from peripheral organs, were silent. Under these conditions, recruitment order is likely to depend on axon caliber, rather than on discharge regularity. Fortunately, in the frog vestibular nerve, axon diameter and discharge regularity are highly correlated (Honrubia et al. 1989). In the isolated brain, two EPSP components are specifically related to the low-threshold activation of thick, presumably irregular fibers. One is a small (0.5–2 mV), short-latency electrical EPSP, recorded from $\approx 30\%$ of secondary neurons. The second is an EPSP mediated by NMDA (N-methyl-D-aspartate) receptors, which is of almost comparable kinetics to the remaining, considerably larger non-NMDA component. Electrical transmission between the vestibular nerve and secondary neurons occurs in birds (Wilson and Wylie 1970; Peusner and Giaume 1994) and may occur in rodents (Wylie 1973). Both NMDA and non-NMDA chemical transmission between these structures is seen in rodents (Kinney et al. 1994; Takahashi et al. 1994). In the latter animals, NMDA transmission is considerably slower than non-NMDA transmission, and evidence is lacking that either electrical or NMDA transmission is specifically related to thick afferents.

The preceding results required intrasomatic recordings of EPSPs, which are technically difficult, especially in intact animals. It would be convenient if recruitment order could be exploited to deduce the regularity of afferent input in experiments where the extracellular discharge of secondary vestibular neurons is recorded. Spike discharges might be expected to have lower thresholds in secondary neurons receiving a predominantly irregular input. Unfortunately, the situation is far from simple. In particular, a secondary neuron typically fires to brief shocks when a small, not necessarily representative fraction of its vestibular-

nerve input is recruited (Goldberg et al. 1987). Almost all VO neurons, for example, fire at shock strengths that only recruit irregular afferents (Goldberg et al. 1994), yet these neurons are known to receive a significant regular input (Highstein et al. 1987; Boyle et al. 1992). The interpretation of the effects of single shocks on the operation of multisynaptic pathways is even more difficult as it raises the need to specify the transformation between synaptic input and firing at several sites (Brontë-Stewart and Lisberger 1994).

Distinguishing afferent inputs by means other than their discharge regularity

—Differences in electrical excitability are related to discharge regularity (Smith and Goldberg 1986). Because of this, electrophysiological paradigms based on such differences can be used to distinguish between regularly and irregularly discharging inputs to secondary neurons, but cannot be used to discriminate between inputs with similar cv^* 's, e.g., between inputs from calyx and irregular dimorphic units or between those from bouton and regular dimorphic fibers (Baird et al. 1988; Lysakowski et al. 1995). Calyx and irregular dimorphic units can be distinguished by their rotational gains (Fig. 7A, C), and this could be used in conjunction with intra-axonal labeling to determine if calyx fibers have distinctive central projections. Another approach is provided by the calcium-binding protein, calretinin. In the vestibular nerve, only calyx fibers are calretinin immunoreactive (Desmadryl and Dechesne 1992; Raymond et al. 1993; Dechesne et al. 1994). In a similar way, the intermediate filament protein peripherin may be a specific marker for small, predominantly bouton fibers (Lysakowski et al. 1999). The usefulness of such markers in tracing the central projections of afferents depends on the afferent labeling not being masked by the presence of the same markers in intrinsic or other extrinsic connections of the vestibular nuclei. Calretinin shows promise in this regard (Kevetter 1996; Kevetter and Leonard 1997), as does peripherin (A. Lysakowski, personal communication). As these markers label afferents from all five end organs, their value would be enhanced if they are combined with focal injections of anterograde tracers into specific organs.

Functional ablation of irregular afferents

Because of the difficulty in interpreting the effects of single shocks on multisynaptic pathways, a second method was devised to exploit differences in electrical excitability of regular and irregular afferents (Minor and Goldberg 1991). Constant currents delivered by way of the perilymphatic space alter vestibular-nerve activity with cathodal currents increasing discharge and anodal currents decreasing it. Furthermore, responses are much larger in irregular than in regular afferents. To obtain a selective and reversible ablation of irregular afferents, large bilateral anodal currents are chosen to be of sufficient magnitude to silence irregular afferents, rendering them unresponsive to head rotations. The same currents reduce the background discharge of regular afferents to a much lesser extent and the latter fibers remain responsive.

Remarkably, the functional ablation of irregular afferents did not affect either the horizontal or vertical angular vestibulo-ocular reflex (AVOR) (Minor and Goldberg 1991; Angelaki and Perachio 1993). Sinusoidal head rotations of 0.5 and 2 Hz, as well as rapid head turns were used. Such rotations exercise the midband and high-frequency AVOR, which presumably relies on the direct, three-neuron VOR pathway. The conclusion that irregular afferents provide only a small input to direct AVOR pathways is consistent with the observation that small eye movements are produced by single shocks that only activate the most irregular afferents (Brontë-Stewart and Lisberger 1994).

The functional-ablation studies imply that direct AVOR pathways do not receive irregular ipsilateral vestibular-nerve (V_i) inputs (Minor and Goldberg 1991; Angelaki and Perachio 1993), while EPSP recordings show that such afferents provide a substantial V_i

monosynaptic input to the pathways' secondary neurons (Highstein et al. 1987; Boyle et al. 1992). One explanation for the apparent discrepancy is that polysynaptic inhibitory pathways could cancel the irregular V_i monosynaptic inputs on the secondary neurons (Minor and Goldberg 1991). Consistent with the suggestion, many secondary neurons show disynaptic V_i inhibitory inputs (Goldberg et al. 1987; Straka and Dieringer 1996) and, at least in the frog, the inhibitory inputs come from the same semicircular canal giving rise to monosynaptic V_i excitatory inputs (Straka et al. 1997).

The possibility of such cancellation was studied in alert monkeys by recording from secondary neurons presumed to contribute to VOR pathways and comparing their discharge in the presence or absence of bilateral ablating currents (Chen-Huang et al. 1997). The currents reduced the background discharge of all neurons, but did not affect the mean gain or phase of their response to 2-Hz sinusoidal head rotations, implying that irregular inputs were either not present or were canceled at the level of the secondary neurons. Evidence for the presence of irregular inputs came from a consideration of individual secondary neurons. While cancellation was nearly perfect on a population basis, individual neurons could have their gains increased or decreased by the currents. The former units are interpreted as receiving a net inhibitory input from irregular afferents; the latter, a net excitatory input from the same afferents. Although population gains were unaltered by the currents, the decrease in background discharge resulted in inhibitory saturation becoming more common. As eye movements were unaffected by the currents, it would appear that the brain can compensate for such inhibitory saturation (Pulaski et al. 1981; Paige 1983). It is unknown how this is accomplished, especially when secondary neurons are silenced.

A presumed function of the polysynaptic inputs converging on secondary neurons is that they could be gated to modify the operation of the VOR under appropriate behavioral circumstances, e.g., during voluntary cancellation of the VOR (Cullen and McCrea 1993; Cullen et al. 1993) or during the viewing of near targets (Viirre et al. 1986; Chen-Huang and McCrea 1999a, 1999b). The increase in the gain of the AVOR during near viewing is reduced by the functional ablation (Chen-Huang and McCrea 1998), as are the eye-movement responses produced by long-duration, constant-velocity head rotations (Angelaki and Perachio 1993) or by off-vertical-axis rotations (OVAR) (Angelaki et al. 1992). Both of the latter two responses involve indirect, velocity-storage circuits acting on canal (Robinson 1977; Raphan et al. 1979) or otolith inputs (Cohen et al. 1983). On the other hand, studies of the effects of the ablating currents on the linear VOR (LVOR) have produced inconsistent results. Chen-Huang and McCrea (1998) studied the eye movements produced during eccentric whole-body rotations, which include both AVOR and LVOR components. They reported that the ablating currents had only small effects and that these could be attributed to changes in the AVOR component. On the other hand, Angelaki et al. (1998; D. E. Angelaki, personal communication) found that anodal currents reduced the sensitivity of the LVOR produced on a linear sled and its dependence on viewing distance, while cathodal currents had the opposite effect. Changes were relatively small and were most pronounced at high frequencies (5–30 Hz).

The logic behind the functional-ablation paradigm deserves some comment. Provided that the bilateral anodal currents are set sufficiently high, they will ablate irregular afferents without silencing regular afferents. Any response unaffected by the ablation procedure presumably does not require irregular afferents. As is almost always the case with ablation paradigms, such “negative” results are easier to interpret than are “positive” results. In particular, it cannot be concluded that a response diminished by the currents necessarily depends on irregular afferents (Chen-Huang et al. 1997; Chen-Huang and McCrea 1998). This is because most responses involve polysynaptic pathways, which can carry regular, irregular, or mixed signals. With the general reduction in afferent activity produced by

anodal currents, even a pathway carrying an exclusively regular signal might be silenced by the currents or by a combination of the currents and vestibular stimulation. To lessen this possibility, the effects of the currents should be tested with small-amplitude vestibular stimuli that minimize silencing. Varying the magnitude and polarity of the currents may also be instructive. So, for example, the response to a vestibular signal that results in inhibitory saturation might be increased by cathodal currents (Angelaki et al. 1998; D. E. Angelaki, personal communication).

Afferent inputs and discharge properties of central vestibular neurons

Central vestibular neurons can differ in their discharge regularity (Iwamoto et al. 1990; Graf et al. 1993; Chen-Huang et al. 1997) and rotational phases (Fuchs and Kimm 1975; Lisberger and Miles 1980; Chubb et al. 1984; Tomlinson and Robinson 1984; McFarland and Fuchs 1992; Scudder and Fuchs 1992; Cullen and McCrea 1993). In this section, we consider the possibility that central neurons reflect their afferent inputs in these discharge properties.

Discharge regularity—Most secondary vestibular neurons receive a convergent input from several vestibular-nerve afferents, with the contribution of each afferent being so small that unitary EPSPs have been difficult to detect (Kawai et al. 1969; S. M. Highstein and J. M. Goldberg, unpublished observations). The incoming impulse traffic reaching a secondary neuron can be likened to the superposition of several, independent renewal processes, in which case the timing of spikes from all sources should approach that of a Poisson process (Cox 1962). This is so whether the discharge of individual input fibers is regular or irregular (Fig. 11A).¹ Hence, there is no reason for secondary or higher-order vestibular neurons to resemble their afferent input in discharge regularity. The conclusion was tested in secondary neurons where ablating currents were used to estimate the relative magnitudes of regular and irregular vestibular-nerve inputs (Chen-Huang et al. 1997). Not surprisingly, it was found that there was no correlation between these estimates and the discharge regularity of central neurons.

As is the case for vestibular-nerve afferents, the discharge regularity of central vestibular neurons is likely to be determined by their intrinsic electrophysiological properties, especially the AHPs triggered by each spike of a repetitive train. In slice preparations, MVN neurons have a background discharge in the apparent absence of synaptic inputs (Serafin et al. 1991a, 1991b; du Lac and Lisberger 1995; Johnston and Dutia 1996) (Fig. 10A, C). Such autochthonous (“pacemaker”) firing is not seen in the intact brain, where the background firing of secondary neurons is abolished when the ipsilateral vestibular nerve is acutely sectioned (Smith and Curthoys 1989; Newlands and Perachio 1990). The source of such activity in slices is unclear. Timing of spikes during “pacemaker” activity is controlled by AHPs (Fig. 10A–D), and firing rate can be modulated by intracellularly injected currents (Fig. 10B, D). Presumably reflecting the lack of quantal synaptic input, the spacing of action potentials in the slice preparation is much more regular than that seen in an in vitro whole-brain preparation (Babalian et al. 1997) or in intact animals (Iwamoto et al. 1990; Graf et al. 1993; Chen-Huang et al. 1997).

Based on the characteristics of their AHPs, most MVN neurons in slice preparations of rodents (Serafin et al. 1991a, 1991b; Johnston et al. 1994; Dutia and Johnston 1998) and in

¹The argument assumes that unitary EPSPs are unaffected by the spacing of action potentials in individual afferents, which is equivalent to assuming that neither facilitation nor depression is an important feature of synaptic transmission between vestibular-nerve afferents and secondary vestibular neurons. In our intracellular studies (Goldberg et al. 1987; Highstein et al. 1987; Boyle et al. 1992), we relied on a paradigm that compared the EPSPs with two identical, closely spaced, near-maximal shocks (Fig. 9). In almost all secondary neurons, the two EPSPs were of comparable magnitude, implying that there was little facilitation or depression

the in vitro whole brain of the same animals (Babalian et al. 1997) can be distinguished into two categories. “A” neurons have a single-component AHP (Fig. 10B), whose approach to the next action potential is delayed by the activation of an A-like K^+ current (Fig. 10A, B). In contrast, “B” units have a double-component AHP showing no evidence of an A current (Fig. 10C, D). In addition to these defining features, the two groups differ in spike width (Fig. 10E), and the presence in some “B” neurons of low-threshold Ca^{2+} spikes and related phenomena (Fig. 10H–J). du Lac and Lisberger (1995) were unable to confirm in the chick that MVN neurons fell into a few, discrete classes based on their electrophysiology.

Two features may bear on the discharge regularity of MVN neurons. First, AHPs are shallower in “B” than in “A” neurons (Fig. 10F, G) and, second, more than half of the “B”, but none of the “A”, neurons have a persistent, subthreshold Na^+ current. Both features might be expected to make the discharge of “B” neurons more irregular than that of “A” neurons. The expectation was only partly confirmed in the in vitro whole brain (Babalian et al. 1997). “A” neurons in this preparation had a relatively regular discharge, while “B” neurons could be regular or irregular. As the authors point out (Vidal et al. 1996), there are several differences between in vitro and in vivo conditions, which suggest caution in the extension of the findings to the latter situation.

It is unlikely that the discharge regularity of secondary neurons reflect their afferent input. In addition, no secondary neuron has a discharge anywhere near as regular as that seen in the most regular vestibular-nerve afferents (Iwamoto et al. 1990; Graf et al. 1993; Chen-Huang et al. 1997). Despite these disclaimers, there is some indication that the discharge regularity of secondary neurons could be of functional importance. In the alert cat, secondary vestibulo-ocular neurons with and without collaterals descending to the obex differed in their discharge regularity (Iwamoto et al. 1990). As is the case for vestibular-nerve afferents, the discharge regularity of secondary neurons may be related to their natural-stimulation gains. Consistent with this idea, the rotational gains of cat VOR neurons were positively correlated with cv^* ; on the other hand, the eye-position sensitivity of the same neurons was not (Iwamoto et al. 1990). There was a positive relation between rotational gain and cv^* among vestibular units with no oculomotor signals recorded in the alert squirrel monkey (Chen-Huang et al. 1997). A similar relation was not evident for the rotational or eye-position responses of secondary neurons carrying both kinds of signals. Since a central neuron can receive several different inputs, it is easy to imagine that its sensitivity to a particular input is related to the weight of the input and that this might obscure any relation to the neuron's intrinsic sensitivity.

Response dynamics—It has been suggested that the rotational phase of central-canal-related neurons might be determined by the response dynamics of their afferents (Tomlinson and Robinson 1984; Iwamoto et al. 1990; Minor and Goldberg 1991). To study this possibility, the rotational phases of secondary neurons were compared in the presence and absence of anodal ablating currents (Chen-Huang et al. 1997). In this way, the phases (Θ_R and Θ_I) contributed by each central neuron's regular (R) and irregular (I) afferent inputs could be estimated. For 2-Hz sinusoidal rotations, irregular afferents lead regular afferents by $\approx 30^\circ$. Were the rotational response of central neurons a linear summation of the two kinds of afferent input, then, in their unperturbed (no-current) discharge, units receiving an irregular inhibitory (I_{INH}) input should phase lag units receiving a comparable excitatory (I_{EXC}) input. Expectations were not confirmed. It was found that the phase of central neurons was unrelated to the sign or magnitude of their irregular afferent inputs. Values of Θ_R for units receiving I_{EXC} inputs and of Θ_I for units receiving I_{INH} inputs were similar to those found in the vestibular nerve. On the other hand, the regular inputs to units with I_{INH} inputs as well as the irregular I_{EXC} inputs were phase advanced by 20–30° from the corresponding afferents.

The findings suggest that central mechanisms can result in differences between the rotational phases of secondary neurons and their afferent inputs. One such mechanism, a fast adaptive process, has been observed in some central vestibular neurons (Ezure et al. 1983; Serafin et al. 1991a) and would produce phase advances.

The vestibular system and sensorimotor integration

The vestibular system is involved in sensorimotor integration to a greater extent than are many other sensory systems. This is evidenced by the presence of three-neuron arcs connecting the ear with motoneurons (Wilson and Maeda 1974; Ito et al. 1977) and of oculomotor signals on second-order relay neurons (Fuchs and Kimm 1975; Lisberger and Miles 1980; Scudder and Fuchs 1992). That the vestibular system sits at an interface between sensory and motor processing is made especially clear by the recent finding that the signals of some secondary relay neurons differ for active and passive head movements (McCrea et al. 1996). It would be surprising if some of the organizational principles of the vestibular system did not reflect its role in sensorimotor integration.

Along these lines, it has been suggested that differences in afferent response dynamics could compensate for the different dynamic loads controlled by vestibuloocular and vestibulospinal reflexes (Fernández and Goldberg 1971; Bilotto et al. 1982). As we have seen, the functional ablation of irregular afferents does not alter the midband or high-frequency AVOR (Minor and Goldberg 1991; Angelaki and Perachio 1993). In contrast, two lines of evidence suggest that the vestibulocollic reflex (VCR) receives a predominantly irregular input.

1. There is a difference in the response dynamics of the VCR evoked by horizontal head rotations (Bilotto et al. 1982) and by sinusoidally modulated galvanic currents (Wilson et al. 1979). Regular afferents have similar response dynamics to natural and galvanic stimulation, but irregular afferents have different response dynamics for the two modes of stimulation (Goldberg et al. 1982; Ezure et al. 1983). Hence, the difference in reflex response dynamics could be explained by a contribution of irregular afferents to the VCR. The argument depends on the assumption that the contributions of central pathways to reflex dynamics are the same for the two stimulation modes. But the assumption may be wrong, especially when one considers that the patterns of afferent activation produced by natural and by galvanic stimulation differ in many other ways besides response dynamics (see Minor and Goldberg 1991 for a discussion).
2. Secondary neurons terminating in the upper cervical spinal cord receive a more irregular afferent input than do those destined for other targets (Boyle et al. 1992). This argument, like the previous one, is not entirely persuasive. In particular, the upper cervical cord also receives collaterals from vestibulospinal neurons destined for lower spinal levels (Rapoport et al. 1977a, 1977b), as well as from VOC neurons projecting both to the oculo-motor nuclei and the spinal cord (Isu and Yokota 1983; Hirai and Uchino 1984; Isu et al. 1988; Minor et al. 1990). Some of these other secondary neurons provide mainly regular inputs (Boyle et al. 1992).

Discharge regularity and sensory coding

Much of this review has been concerned with the role played by different afferent contingents in the organization of central vestibular pathways. Information transmission from vestibular-nerve afferents to secondary neurons provides another perspective. In particular, the following question arises: does an irregular afferent offer any advantage in the encoding of sensory information or in its transmission to secondary neurons?

In considering this question, it will be supposed that information is represented as the discharge rate, λ , averaged over some period, Δt . Because of the larger fluctuations in its intervals, an irregular afferent will require a longer period than a regular unit to estimate λ with a given degree of precision (Goldberg et al. 1984; Myers and Lewis 1990). An irregular unit, although less efficient in the encoding of steady-state information, may offer advantages in the handling of dynamic stimuli. A regular unit can preserve waveform information when the stimulus frequency bandwidth is less than λ . An irregular unit can preserve such information over a larger bandwidth (Geisler 1968; Stein 1970; Stein et al. 1972). While this conclusion may provide a rationale as to why, for example, auditory afferents are irregular, it is of limited applicability in dealing with vestibular-nerve fibers, which typically have discharge rates of 50–150 spikes/s in mammals (Goldberg and Fernández 1971a; Fernández and Goldberg 1976a; Baird et al. 1988; Goldberg et al. 1990a), much higher than the ≈ 10 -Hz bandwidth of naturally occurring head movements (Grossman et al. 1988).

In vestibular-nerve afferents, an irregular discharge is related to the enhanced sensitivity of the afferent terminal's spike encoder. It seems plausible that larger gains could improve information transmission to secondary neurons. To consider the subject, we designate $m(\Delta t)$ as the number of spikes occurring in Δt and suppose that there is a linear stimulus-response relation between $m(\Delta t)$ and the appropriate stimulus dimension, x . Let $S_m^2(\Delta t)$ be the signal power, i.e., the variance in $m(\Delta t)$ as associated with S_x^2 , the variance in $S_m^2(\Delta t) = g^2 S_x^2(\Delta t) t^2 = S_\lambda^2 \Delta t^2$, where g is the afferent gain in spikes·s⁻¹/x and S_λ^2 is the signal-related variance in the discharge rate, λ . $N_m^2(\Delta t)$ is the noise power, i.e., the variance in $m(\Delta t)$ associated with interspike-interval variability. If both the signal and the noise are gaussian distributed, the information rate in bits/s encoded by a single afferent during Δt is given by Shannon's (1948; Fano 1961) formula²:

$$I(\Delta t) = W \log_2 \left[1 + \frac{S_m^2(\Delta t)}{N_m^2(\Delta t)} \right] \cong W \log_2 \left[1 + \frac{S_m^2(\Delta t)}{N_m^2(\Delta t)} \right] \quad (1)$$

where W is the bandwidth of the signal. $\Delta t = 1/2W$ is chosen based on the sampling theorem (Shannon 1949; Fano 1961), which states that a band-limited signal can be represented by $2W$ independent, equally spaced points per second. Application of eq. 1 or be a constant, $\bar{N}_m^2(\Delta t)$. In the approximation, we set $\bar{N}_m^2(\Delta t)$ to a value appropriate to the mean (resting) rate, $\bar{\lambda}$

To study the influence of discharge regularity on information encoding, it is assumed that the afferent interval distributions have the probability densities

$$p(u) = \frac{\rho(\rho u)^{\alpha-1} e^{-\rho u}}{(\alpha-1)!} \quad (2)$$

of gamma distributions of integral order, α , and mean rate, ρ/α . Such distributions range from an exponential distribution, indicating a random (Poisson) process ($\alpha=1$), to a Dirac delta distribution, indicating a completely regular discharge ($\alpha \rightarrow \infty$). In general, $cv = 1/\sqrt{\alpha}$

²The approach used in estimating the information contained in afferent spike trains is similar to that described by Stein (1967). In calculating information capacities, he assumed that stimulus (and response) probabilities were uniformly distributed, which maximizes the capacity for a fixed *range*. I have assumed that the probabilities are normally distributed, which maximizes capacity for a specified *variance*. My preference is based on the relative simplicity it provides in comparing the information contained in spike trains and postsynaptic voltages. The treatment of postsynaptic voltages bears some resemblance to the linear decoding of Bialek et al. (1991; Bialek and Rieke 1992)

(Fig. 11B). It should be emphasized that eq. 2 was chosen because it provides a convenient set of interval distributions, not because it provides the basis for a realistic model of repetitive discharge.³

$\bar{N}_m(\Delta t)$ increases as cv increases from 0.023 to unity (Fig. 11C). The increase (●--●, Fig. 11C), particularly for small cv's, is more gradual than that predicted by the asymptotically linear approximation to $\bar{N}_m(\Delta t)$ (--, Fig. 11C). (How the increase in $\bar{N}_m(\Delta t)$ affects $I(\Delta t)$ for individual afferents will depend on the relation between gain and cv or, equivalently, on the relation between $S_m(\Delta t)$ and cv. Results are presented in Fig. 11D for $\Delta t=50$ ms, which is the sampling interval for a bandwidth $W=10$ Hz. The rms stimulus magnitude, S_x , was limited to 20°/s to minimize inhibitory silencing (see Fig. 11 legend for details). When gain or $S_m(\Delta t)$ is constant, there is a decline in $I(\Delta t)$ as cv increases (●--●, Fig. 11D). Were there an increase in gain paralleling the increase in $\bar{N}_m(\Delta t)$, $I(\Delta t)$ would be unaffected by cv. For dimorphic units, the gain increases linearly with cv (Fig. 7A). Under these circumstances, there is an increase in $I(\Delta t)$ with cv (○--○, Fig. 11D). Corresponding values of $I(\Delta t)$ for individual calyx units are small, reflecting the combination of a small $S_m(\Delta t)$ and a large $\bar{N}_m(\Delta t)$ (Fig. 11D, ● and ○).

Of particular interest is the situation where several afferents converge on a secondary neuron. As was already pointed out, the impulse traffic arriving at the neuron approaches a Poisson process whether the separate afferents are regular or irregular. Suppose that n afferents converge on the neuron and that the resting rate, averaged across all afferents, is $\bar{\lambda}$.

The expected number of spikes in Δt is $\bar{\lambda}\Delta t$. Then $\bar{N}_{m,n}(\Delta t) = n\bar{\lambda}\Delta t$ and $\bar{S}_{m,n}^2(\Delta t) = n^2 S_m^2(\Delta t) = n^2 S_\lambda^2 \Delta t^2$. The first relation follows from the fact that, for a Poisson process, the variance in the number of events and the mean number of events are equal. When there are n inputs, the signal $S_{m,n}$ increases n -fold. Hence,

$$S_{m,n}^2(\Delta t) / \bar{N}_{m,n}^2(\Delta t) = n S_\lambda^2 \Delta t / \bar{\lambda} \quad (3)$$

Note that the signal-to-noise ratio and, hence, $I(\Delta t)$ depend on $\bar{S}_\lambda^2(\Delta t)$, but not on discharge regularity.

Figure 11D (■--■) depicts the situation when several dimorphic afferents converge on a secondary neuron. The information, $I(\Delta t)$, contained in the superimposed (pooled) discharge is plotted against the average value of cv for the afferents. Because of the linear relation between $S_m(\Delta t)$ and cv for individual dimorphic afferents, there is an increase in $I(\Delta t)$ as the average cv increases. Also included in the figure is the corresponding $I(\Delta t)$ when the inputs, which are each assumed to have identical discharge properties, are kept separate (Fig. 11D, □--□). From the difference between the "pooled" and "separate" curves, it can be seen that convergence results in a loss of information. The loss is smaller, the more irregular the discharge and disappears for a Poisson process (cv=1, not shown). The same calculations are done for calyx units and are shown as separate points in Fig. 11D (●, ○). Because of their relatively low gains, calyx units transmit much less information than do irregular dimorphic units.

³A gamma distribution of order α is the cumulative waiting-time distribution for α successive occurrences of a Poisson-distributed variable (Cox 1962), which would be the appropriate interval distribution for an integrate-and-fire neuron requiring α inputs to reach firing threshold. Such a model is inadequate because it does not consider the decay of individual EPSPs at the synapses between hair cells and afferent terminals (Furukawa 1978; Rossi et al. 1994)

In the preceding paragraph, we have considered the information encoded in the pooled discharge of the afferents converging on a secondary neuron. We now show that a similar amount of information can be transmitted to the secondary neuron in the form of postsynaptic voltages. The point is important in establishing that there need be little loss in the information delivered to the secondary neuron. Because the incoming impulse traffic approaches a Poisson process, shot-noise theory is applicable (Rice 1944). Let the EPSP generated by an input at $t=t_K$ be described by a time function, $h(t-t_K)$, which is identically zero for $t < t_K$. From Campbell's theorem,

$$\begin{aligned} S_{V,n} &= nS_\lambda \int_0^\infty h(u) du = nS_\lambda I_1 \\ \overline{N}_{V,n}^2 &= n\lambda \int_0^\infty h^2(u) du = \lambda I_2 \end{aligned} \quad (4)$$

Here, $S_{V,n}$ is the mean value of the instantaneous voltage (V) and $\overline{N}_{V,n}$ is the rms value of the fluctuations about $S_{V,n}$. As both $S_{V,n}$ and $\overline{N}_{V,n}$ are gaussian distributed (Rice 1944), the information should be proportional to $\log_2 \left(1 + S_{V,n}^2 / \overline{N}_{V,n}^2 \right)$. Most simply shaped EPSPs can be fit by a function, $h(t) = A(\alpha t)^p \exp(-\alpha t)$ (see, for example, Jack et al. 1983; Rossi et al. 1994). In addition, the function allows the two integrals in eq. 4 to be expressed in terms of complete gamma functions, i.e., $I_1 = A\Gamma(p+1)/\alpha$ and $I_2 = A^2\Gamma(2p+1)/(2^{2p+1}\alpha)$, where

$$\begin{aligned} \Gamma(p) &= \int_0^\infty t^{p-1} e^{-t} dt \\ &= \alpha^p \int_0^\infty t^{p-1} e^{-\alpha t} dt \end{aligned} \quad (5)$$

Assuming that the voltage is averaged over $f_s \Delta t$ equally-spaced samples during Δt ,

$$\begin{aligned} S_{V,n}^2(\Delta t) / \overline{N}_{V,n}^2(\Delta t) &= 2^{2p+1} f_s \Delta t n S_\lambda^2 \Gamma^2(p+1) / 2\pi f_c \lambda (2p+1) \\ &= \kappa n S_\lambda^2 \Delta t / \lambda \end{aligned} \quad (6)$$

where $\kappa = 2^{2p+1} f_s \Gamma^2(p+1) / 2\pi f_c \Gamma(2p+1)$ and $2\pi f_c = \alpha$. The signal-to-noise ratio parallels that in eq. 3. Values of the two ratios will equal one another ($K=1$) when $f_s = 2f_c$ and $p=0.5$.⁴

Concluding remarks

In the somatosensory and visual systems, distinct populations of sensory axons innervating a single sensory surface project to separate sets of central neurons. One result of the parallel projections is that the discharge properties of central neurons resemble those of their afferent inputs. A similar situation occurs in the vestibular system, where parallel pathways interconnect the several peripheral organs with various oculomotor and spinal motoneuron pools. This paper reviews the possibility that distinct sets of afferents innervating individual organs and distinguished among other ways by their discharge regularity give rise to segregated central pathways. Intracellular recordings of EPSPs show that the direct vestibular-nerve input to most secondary neurons consists of a mixture of regular and irregular afferents. In addition, functional-ablation studies indicate that the rotational phases of secondary neurons need not resemble those of their afferent inputs. This last finding implies that some of the regular and/or irregular inputs to secondary neurons are modified by central mechanisms, presumably involving polysynaptic inputs from the vestibular nuclei, cerebellum, and other parts of the brain stem. In addition, the intrinsic

⁴It might appear that the signal-to-noise ratio and, hence, $I(\Delta t)$ could be increased without limit by increasing the sampling frequency, f_s . That this is not the case is suggested by the following consideration. The power spectrum of the postsynaptic signal has a bandwidth, f_c . As f_s increases beyond $2f_c$, the so-called Nyquist frequency, the $f_s \Delta t$ samples are no longer statistically independent and individual samples will provide a declining amount of information (Shannon 1949; Fano 1961)

electrophysiological properties of central neurons may help to shape their responses. In the introduction, we compared the discharge properties of peripheral afferents and secondary neurons in several sensory systems. In terms of possible central modifications of the afferent inputs to secondary neurons, the vestibular pathways would seem to more closely resemble the auditory than the visual or somatosensory systems.

The discharge properties of regular and irregular afferents are so different that it would be surprising if they did not make distinctive contributions to vestibular function. Several suggestions have been considered.

1. Given differences in their response dynamics, regular and irregular afferents could compensate for differences in the dynamic loads represented by various reflexes (Fernández and Goldberg 1971; Bilotto et al. 1982; Boyle et al. 1992) or by individual reflexes operating in different parts of their frequency range (Angelaki et al. 1998; D. E. Angelaki, personal communication).
2. Irregular inputs to secondary VOR neurons may be gated to modify the operation of reflexes under varying behavioral circumstances (Angelaki et al. 1998; Chen-Huang and McCrea 1998).
3. In their directional properties, otolith afferents can be characterized by a one-dimensional vector (Fernández and Goldberg 1976a; Dickman et al. 1991). In contrast, some central otolith neurons show a two-dimensional sensitivity that might be explained by the neurons receiving a convergent input from two sets of afferents differing in their response dynamics and directional properties (Angelaki et al. 1993; Bush et al. 1993). Because they differ in their response dynamics, one of the sets could be regular, while the other set could be irregular.
4. Calyx afferents have relatively low gains compared with irregular dimorphic afferents. This may serve to expand the stimulus range over which the response of calyx afferents remains linear, while at the same time preserving other features peculiar to irregular afferents. Among those features are phasic response dynamics and large responses to efferent activation.
5. Because of the convergence of several afferents onto each secondary neuron, information transmission to the latter depends on the gain of individual afferents, but not on their discharge regularity. Among dimorphic units, gain increases in parallel with the normalized coefficient of variation, cv^* , and this should improve information transmission to secondary neurons.

Definitive evidence is lacking for each of these suggestions. Hopefully, the situation will be clarified in the not too distant future.

Acknowledgments

A. Lysakowski, V. J. Wilson, and an anonymous reviewer made helpful comments on the manuscript. The author's research is supported by NIH grants DC 02508 and DC 03946.

References

- Aitkin, LM.; Irvine, DRF.; Webster, WR. Central neural mechanisms of hearing. In: Darian-Smith, I., editor. Handbook of physiology. Section I. The nervous system. Volume III. Sensory processes, Part 2. Williams & Wilkins; Baltimore: 1984. p. 675-737.
- Angelaki DE, Perachio AA. Contribution of irregular semicircular canal afferents to the horizontal vestibuloocular response during constant velocity rotation. *J Neurophysiol.* 1993; 69:996-999. [PubMed: 8385205]

- Angelaki DE, Perachio AA, Mustari MJ, Strunk CL. Role of irregular otolith afferents in the steady-state nystagmus during off-vertical axis rotation. *J Neurophysiol.* 1992; 68:1895–1900. [PubMed: 1479452]
- Angelaki DE, Bush GA, Perachio AA. Two-dimensional spatiotemporal coding of linear acceleration in vestibular nuclei neurons. *J Neurosci.* 1993; 13:1403–1417. [PubMed: 8463828]
- Angelaki DE, McHenry MQ, Perachio AA, Dickman JD. Irregular otolith afferent inputs to the translational vestibuloocular reflex. *Soc Neurosci Abstr.* 1998; 24:1411.
- Babalian A, Vibert N, Assie G, Serafin M, Muhlethaler M, Vidal PP. Central vestibular networks in the guinea-pig: functional characterization in the isolated whole brain in vitro. *Neuroscience.* 1997; 81:405–426. [PubMed: 9300431]
- Baird RA, Desmadryl G, Fernández C, Goldberg JM. The vestibular nerve of the chinchilla. II. Relation between afferent response properties and peripheral innervation patterns in the semicircular canals. *J Neurophysiol.* 1988; 60:182–203. [PubMed: 3404216]
- Barrett EF, Barrett JN. Separation of two voltage-sensitive potassium currents and demonstration of a tetrodotoxin-resistant calcium current in frog motoneurons. *J Physiol.* 1976; 255:737–774. [PubMed: 1083431]
- Bialek W, Rieke F. Reliability and information transmission in spiking neurons. *Trends Neurosci.* 1992; 15:428–434. [PubMed: 1281349]
- Bialek W, Rieke F, de Ruyter van Steveninck RR, Warland D. Reading a neural code. *Science.* 1991; 252:1854–1857. [PubMed: 2063199]
- Bilotto G, Goldberg J, Peterson BW, Wilson VJ. Dynamic properties of vestibular reflexes in the decerebrate cat. *Exp Brain Res.* 1982; 47:343–352. [PubMed: 7128706]
- Boyle R, Highstein SM. Resting discharge and response dynamics of horizontal semicircular canal afferents of the toadfish, *Opsanus tau*. *J Neurosci.* 1990a; 10:1557–1569. [PubMed: 2332797]
- Boyle R, Highstein SM. Efferent vestibular system in the toadfish: action upon horizontal semicircular canal afferents. *J Neurosci.* 1990b; 10:1570–1582. [PubMed: 2332798]
- Boyle R, Carey JP, Highstein SM. Morphological correlates of response dynamics and efferent stimulation in horizontal semicircular canal afferents of the toadfish, *Opsanus tau*. *J Neurophysiol.* 1991; 66:1504–1521. [PubMed: 1765791]
- Boyle R, Goldberg JM, Highstein SM. Inputs from regularly and irregularly discharging vestibular nerve afferents to secondary neurons in squirrel monkey vestibular nuclei. III. Correlation with vestibulospinal and vestibuloocular output pathways. *J Neurophysiol.* 1992; 68:471–484. [PubMed: 1527570]
- Brichta AM, Goldberg J. Afferent and efferent responses from morphological fiber classes in the turtle posterior crista. *Ann NY Acad Sci.* 1996; 781:183–195. [PubMed: 8694414]
- Brichta, AM.; Goldberg, JM. Voltage responses of hair cells from the turtle posterior crista to sinusoidal electric currents. Abstracts, 21st Midwinter Meeting. Association for Research in Otolaryngology; 1998. p. 24
- Brichta AM, Goldberg JM. Morphological identification of physiologically characterized afferents innervating the turtle posterior crista. *J Neurophysiol.* 2000a in press.
- Brichta AM, Goldberg JM. Responses to electrical stimulation of efferent fibers and excitatory response-intensity relations of afferents innervating the turtle posterior crista. *J Neurophysiol.* 2000b in press.
- Brichta AM, Peterson EH. Functional architecture of vestibular primary afferents from the posterior semicircular canal of a turtle, *Pseudemys (Trachemys) scripta elegans*. *J Comp Neurol.* 1994; 344:481–507. [PubMed: 7929889]
- Brichta, AM.; Eatock, RA.; Goldberg, JM. Characterization of the I_{KL} outward current in hair cells from the turtle posterior crista. Abstracts, 21st Midwinter Meeting. Association for Research in Otolaryngology; 1998. p. 24
- Brontë-Stewart HM, Lisberger SG. Physiological properties of vestibular primary afferents that mediate motor learning and normal performance of the vestibulo-ocular reflex in monkeys. *J Neurosci.* 1994; 14:1290–1308. [PubMed: 8120625]

- Bush GA, Perachio AA, Angelaki DE. Encoding of head acceleration in vestibular neurons. I. Spatiotemporal response properties to linear acceleration. *J Neurophysiol.* 1993; 69:2039–2055. [PubMed: 8350132]
- Chen-Huang C, McCrea RA. Contribution of vestibular nerve irregular afferents to viewing distance-related changes in the vestibulo-ocular reflex. *Exp Brain Res.* 1998; 119:116–130. [PubMed: 9521542]
- Chen-Huang C, McCrea RA. Effects of viewing distance on the responses of horizontal canal-related secondary vestibular neurons during angular head velocity. *J Neurophysiol.* 1999a; 81:2517–2537. [PubMed: 10322087]
- Chen-Huang C, McCrea RA. Effects of viewing distance on the responses of vestibular neurons to combined angular and linear vestibular stimulation. *J Neurophysiol.* 1999b; 81:2538–2557. [PubMed: 10322088]
- Chen-Huang C, McCrea RA, Goldberg JM. Contributions of regularly and irregularly discharging vestibular-nerve inputs to the discharge of central vestibular neurons in the alert squirrel monkey. *Exp Brain Res.* 1997; 114:405–422. [PubMed: 9187277]
- Chubb MC, Fuchs AF, Scudder CA. Neuron activity in monkey vestibular nuclei during vertical vestibular stimulation and eye movements. *J Neurophysiol.* 1984; 52:724–742. [PubMed: 6333490]
- Cohen B, Suzuki J-I, Bender MB. Eye movements from semicircular canal stimulation in the cat. *Ann Otol.* 1964; 73:153–169.
- Cohen B, Suzuki J-I, Raphan T. Role of the otolith organs in generation of horizontal nystagmus: effects of selective labyrinthine lesions. *Brain Res.* 1983; 276:159–164. [PubMed: 6626994]
- Connor JA. Slow repetitive activity from fast conductance changes in neurons. *Fed Proc.* 1978; 37:2139–2145. [PubMed: 658453]
- Correia MJ, Lang DG. An electrophysiological comparison of solitary type I and type II vestibular hair cells. *Neurosci Lett.* 1990; 116:106–111. [PubMed: 2259440]
- Cox, DR. *Renewal theory.* Wiley; New York: 1962.
- Cullen KE, McCrea RA. Firing behavior of brain stem neurons during voluntary cancellation of the horizontal vestibuloocular reflex. I. Secondary vestibular neurons. *J Neurophysiol.* 1993; 70:828–843. [PubMed: 8410175]
- Cullen KE, Chen-Huang C, McCrea RA. Firing behavior of brain stem neurons during voluntary cancellation of the horizontal vestibuloocular reflex. II. Eye movement related neurons. *J Neurophysiol.* 1993; 70:844–856. [PubMed: 8410176]
- Darian Smith, I. The sense of touch: performance and peripheral processes. In: Darian-Smith, I., editor. *Handbook of physiology.* Section I. The nervous system. Volume III. Sensory processes, Part 2. Williams & Wilkins; Baltimore: 1984. p. 739-788.
- Dechesne CJ, Rabejac D, Desmadryl G. Development of calretinin immunoreactivity in the mouse inner ear. *J Comp Neurol.* 1994; 346:517–529. [PubMed: 7983242]
- Desmadryl G, Dechesne CJ. Calretinin immunoreactivity in chinchilla and guinea pig vestibular end organs characterizes the calyx unit subpopulation. *Exp Brain Res.* 1992; 89:105–108. [PubMed: 1601088]
- Dickman JD, Angelaki DE, Correia MJ. Response properties of gerbil otolith afferents to small angle pitch and roll tilts. *Brain Res.* 1991; 556:303–310. [PubMed: 1933362]
- du Lac S, Lisberger SG. Membrane and firing properties of avian medial vestibular nucleus neurons in vitro. *J Comp Physiol A.* 1995; 176:641–651. [PubMed: 7769566]
- Dutia MB, Johnston AR. Development of action potentials and apamin-sensitive after-potentials in mouse vestibular nucleus neurones. *Exp Brain Res.* 1998; 118:148–154. [PubMed: 9547083]
- Dykes RW, Landry P, Hicks TP, Diadori P, Metherate R. Specificity of connections in the ventroposterior nuclei of the thalamus. *Prog Neurobiol.* 1988; 30:87–103. [PubMed: 3275408]
- Ezure K, Cohen MS, Wilson VJ. Response of cat semicircular canal afferents to sinusoidal polarizing currents: implications for input-output properties of second-order neurons. *J Neurophysiol.* 1983; 49:639–648. [PubMed: 6834091]
- Fano, RM. *Transmission of information. A statistical theory of communications.* MIT Press; Cambridge: 1961.

- Fernández C, Goldberg JM. Physiology of peripheral neurons innervating semicircular canals of the squirrel monkey. II. Response to sinusoidal stimulation and dynamics of peripheral vestibular system. *J Neurophysiol.* 1971; 34:661–675. [PubMed: 5000363]
- Fernández C, Goldberg JM. Physiology of peripheral neurons innervating otolith organs of the squirrel monkey. I. Response to static tilts and to long-duration centrifugal force. *J Neurophysiol.* 1976a; 39:970–984. [PubMed: 824412]
- Fernández C, Goldberg JM. Physiology of peripheral neurons innervating otolith organs of the squirrel monkey. III. Response dynamics. *J Neurophysiol.* 1976b; 39:996–1008. [PubMed: 824414]
- Fernández C, Baird RA, Goldberg JM. The vestibular nerve of the chinchilla. I. Peripheral innervation patterns in the horizontal and superior semicircular canals. *J Neurophysiol.* 1988; 60:167–181. [PubMed: 3404215]
- Fernández C, Goldberg JM, Baird RA. The vestibular nerve of the chinchilla. III. Peripheral innervation patterns in the utricular macula. *J Neurophysiol.* 1990; 63:767–780. [PubMed: 2341875]
- Fernández C, Lysakowski A, Goldberg JM. Hair-cell counts and afferent innervation patterns in the cristae ampullares of the squirrel monkey with a comparison to the chinchilla. *J Neurophysiol.* 1995; 73:1253–1269. [PubMed: 7608769]
- Fuchs AF, Kimm J. Unit activity in vestibular nucleus of the alert monkey during horizontal angular acceleration and eye movement. *J Neurophysiol.* 1975; 38:1140–1161. [PubMed: 809547]
- Furukawa T, Hayashida Y, Matsuura S. Quantal analysis of the size of excitatory post-synaptic potentials at synapses between hair cells and afferent nerve fibres in goldfish. *J Physiol.* 1978; 276:211–226. [PubMed: 206683]
- Geisler CD. A model of the peripheral auditory system responding to low-frequency tones. *Biophys J.* 1968; 8:1–15. [PubMed: 5641401]
- Goldberg JM, Brichta AM. Evolutionary trends in the of the vertebrate crista ampullaris. *Otolaryngol Head Neck Surg.* 1998; 119:165–171. [PubMed: 9743072]
- Goldberg JM, Fernández C. Physiology of peripheral neurons innervating semicircular canals of the squirrel monkey. I. Resting discharge and response to constant angular accelerations. *J Neurophysiol.* 1971a; 34:635–660. [PubMed: 5000362]
- Goldberg JM, Fernández C. Physiology of peripheral neurons innervating semicircular canals of the squirrel monkey. III. Variations among units in their discharge properties. *J Neurophysiol.* 1971b; 34:676–684. [PubMed: 5000364]
- Goldberg JM, Fernández C. Conduction times and background discharge of vestibular afferents. *Brain Res.* 1977; 122:545–550. [PubMed: 402981]
- Goldberg JM, Fernández C. Efferent vestibular system in the squirrel monkey: anatomical location and influence on afferent activity. *J Neurophysiol.* 1980; 43:986–1025. [PubMed: 6767000]
- Goldberg JM, Fernández C, Smith CE. Responses of vestibular-nerve afferents in the squirrel monkey to externally applied galvanic currents. *Brain Res.* 1982; 252:156–160. [PubMed: 6293651]
- Goldberg JM, Smith CE, Fernández C. Relation between discharge regularity and responses to externally applied galvanic currents in vestibular nerve afferents of the squirrel monkey. *J Neurophysiol.* 1984; 51:1236–1256. [PubMed: 6737029]
- Goldberg JM, Highstein SM, Moschovakis AK, Fernández C. Inputs from regularly and irregularly discharging vestibular nerve afferents to secondary neurons in the vestibular nuclei of the squirrel monkey. I. An electrophysiological analysis. *J Neurophysiol.* 1987; 58:700–718. [PubMed: 3681391]
- Goldberg JM, Desmadryl G, Baird RA, Fernández C. The vestibular nerve of the chinchilla. IV. Discharge properties of utricular afferents. *J Neurophysiol.* 1990a; 63:781–790. [PubMed: 2341876]
- Goldberg JM, Desmadryl G, Baird RA, Fernández C. The vestibular nerve of the chinchilla. V. Relation between afferent discharge properties and peripheral innervation patterns in the utricular macula. *J Neurophysiol.* 1990b; 63:791–804. [PubMed: 2341877]
- Goldberg JM, Lysakowski A, Fernández C. Morphophysiological and ultrastructural studies in the mammalian cristae ampullares. *Hear Res.* 1990c; 49:89–102. [PubMed: 2292511]

- Goldberg, JM.; McCrea, RA.; Chen-Huang, C.; Belton, TM. Central projections of the vestibular nerve. In: Fuchs, A.; Brandt, T.; Büttner, U.; Zee, D., editors. Contemporary ocular motor and vestibular research: a tribute to David A. Robinson. Thieme; Stuttgart: 1994. p. 446-452.
- Graf W, Baker JF, Peterson BW. Sensorimotor transformation in the cat's vestibuloocular reflex system. I. Neuronal signals coding spatial coordination of compensatory eye. *J Neurophysiol.* 1993; 70:2425–2441. [PubMed: 8120591]
- Grossman GE, Leigh RJ, Abel LA, Lanska DJ, Thurston SE. Frequency and velocity of rotational head perturbations during locomotion. *Exp Brain Res.* 1988; 70:470–476. [PubMed: 3384048]
- Hackney CM. Anatomical features of the auditory pathway from cochlea to cortex. *Br Med Bull.* 1987; 43:780–801. [PubMed: 3329925]
- Highstein SM, Politoff AL. Relation of interspike baseline activity to the spontaneous discharges of primary afferents from the labyrinth of the toadfish, *Opsanus tau*. *Brain Res.* 1978; 150:182–187. [PubMed: 208713]
- Highstein SM, Goldberg JM, Moschovakis AK, Fernández C. Inputs from regularly and irregularly discharging vestibular nerve afferents to secondary neurons in the vestibular nuclei of the squirrel monkey. II. Correlation with output pathways of secondary neurons. *J Neurophysiol.* 1987; 58:719–738. [PubMed: 2445938]
- Highstein SM, Rabbitt RD, Boyle R. Determinants of semicircular canal afferent response dynamics in the toadfish, *Opsanus tau*. *J Neurophysiol.* 1996; 75:575–596. [PubMed: 8714636]
- Hille, B. Ionic channels of excitable membranes. 2nd edn.. Sinauer; Sunderland: 1992.
- Hirai N, Uchino Y. Floccular influence on excitatory relay neurons of vestibular reflexes of anterior semicircular canal origin in the cat. *Neurosci Res.* 1984; 1:327–340. [PubMed: 6536901]
- Honrubia V, Hoffman LF, Sitko S, Schwartz IR. Anatomic and physiological correlates in bullfrog vestibular nerve. *J Neurophysiol.* 1989; 61:688–701. [PubMed: 2786056]
- Huwe JA, Peterson EH. Differences in the brain stem terminations of large- and small-diameter vestibular primary afferents. *J Neurophysiol.* 1995; 74:1362–1366. [PubMed: 7500159]
- Iggo A, Muir AR. The structure and function of a slowly adapting touch corpuscle in hairy skin. *J Physiol.* 1969; 200:763–796. [PubMed: 4974746]
- Iso N, Yokota J. Morphophysiological study on the divergent projection of axon collaterals of medial vestibular nucleus neurons in the cat. *Exp Brain Res.* 1983; 53:151–162. [PubMed: 6673993]
- Iso N, Uchino Y, Nakashima H, Satoh S, Ichikawa T, Watanabe S. Axonal trajectories of posterior canal-activated secondary vestibular neurons and their coactivation of extraocular and neck flexor motoneurons in the cat. *Exp Brain Res.* 1988; 70:181–191. [PubMed: 3402563]
- Ito M, Nisimaru N, Yamamoto M. Specific patterns of neuronal connexions involved in the control of the rabbit's vestibulo-ocular reflexes by the cerebellar flocculus. *J Physiol.* 1977; 265:833–854. [PubMed: 300801]
- Iwamoto Y, Kitama T, Yoshida K. Vertical eye movement-related secondary vestibular neurons ascending in medial longitudinal fasciculus in cat. I. Firing properties and projection pathways. *J Neurophysiol.* 1990; 63:902–917. [PubMed: 2341885]
- Jack, JJB.; Noble, D.; Tsien, RW. Electric current flow in excitable cells. Oxford University Press; London: 1983.
- Johnson KO, Hsiao SS. Neural mechanisms of tactual form and texture perception. *Annu Rev Neurosci.* 1992; 15:227–250. [PubMed: 1575442]
- Johnston AR, Dutia MB. Postnatal development of spontaneous tonic activity in mouse medial vestibular nucleus neurones. *Neurosci Lett.* 1996; 219:17–20. [PubMed: 8961293]
- Johnston AR, MacLeod NK, Dutia MB. Ionic conductances contributing to spike repolarization and after-potentials in rat medial vestibular nucleus neurones. *J Physiol.* 1994; 481:61–77. [PubMed: 7531769]
- Jørgensen JM. The sensory epithelia of the inner ear of two turtles, *Testudo graeca* L. and *Pseudemys scripta* (Schoepff). *Acta Zool (Stockh).* 1974; 55:289–298.
- Kawai N, Ito M, Nozue M. Postsynaptic influences on the vestibular non-Deiters nuclei from primary vestibular nerve. *Exp Brain Res.* 1969; 8:190–200. [PubMed: 5808758]

- Kernell D. The repetitive impulse discharge of a simple neurone model compared to that of spinal motoneurons. *Brain Res.* 1968; 11:685–687. [PubMed: 5712015]
- Kevetter GA. Pattern of selected calcium-binding proteins in the vestibular nuclear complex of two rodent species. *J Comp Neurol.* 1996; 365:575–584. [PubMed: 8742303]
- Kevetter GA, Leonard RB. Use of calcium-binding proteins to map inputs in vestibular nuclei of the gerbil. *J Comp Neurol.* 1997; 386:317–327. [PubMed: 9295155]
- Kinney GA, Peterson BW, Slater NT. The synaptic activation of N-methyl-D-aspartate receptors in the rat medial vestibular nucleus. *J Neurophysiol.* 1994; 72:1588–1595. [PubMed: 7823088]
- Li J, Young ED. Discharge-rate dependence of refractory behavior of cat auditory-nerve fibers. *Hear Res.* 1993; 69:151–162. [PubMed: 8226336]
- Lieberman MC. Single-neuron labeling in the cat auditory nerve. *Science.* 1982; 216:1239–1241. [PubMed: 7079757]
- Lieberman MC. Central projections of auditory-nerve fibers of differing spontaneous rate. I. Anteroventral cochlear nucleus. *J Comp Neurol.* 1991; 313:240–258. [PubMed: 1722487]
- Lieberman MC. Central projections of auditory nerve fibers of differing spontaneous rate. II: Posteroventral and dorsal cochlear nuclei. *J Comp Neurol.* 1993; 327:17–36. [PubMed: 8432906]
- Lisberger SG, Miles FA. Role of primate medial vestibular nucleus in long-term adaptive plasticity of vestibuloocular reflex. *J Neurophysiol.* 1980; 43:1725–1745. [PubMed: 6967953]
- Lisberger SG, Pavelko TA, Broussard DM. Responses during eye movements of brain stem neurons that receive mono-synaptic inhibition from the flocculus and ventral paraflocculus in monkeys. *J Neurophysiol.* 1994a; 72:909–927. [PubMed: 7983546]
- Lisberger SG, Pavelko TA, Broussard DM. Neural basis for motor learning in the vestibuloocular reflex of primates. I. Changes in the responses of brain stem neurons. *J Neurophysiol.* 1994b; 72:928–953. [PubMed: 7983547]
- Lysakowski A. Synaptic organization of the crista ampullaris in vertebrates. *Ann NY Acad Sci.* 1996; 781:164–182. [PubMed: 8694413]
- Lysakowski A, Goldberg JM. A regional ultrastructural analysis of the cellular and synaptic architecture in the chinchilla cristae ampullares. *J Comp Neurol.* 1997; 389:419–443. [PubMed: 9414004]
- Lysakowski A, Minor LB, Fernández C, Goldberg JM. Physiological identification of morphologically distinct afferent classes innervating the cristae ampullares of the squirrel monkey. *J Neurophysiol.* 1995; 73:1270–1281. [PubMed: 7608770]
- Lysakowski A, Alonto A, Jacobson L. Peripherin immunoreactivity labels small diameter vestibular 'bouton' afferents in rodents. *Hearing Res.* 1999; 133:149–154.
- Matthews PBC, Stein RB. The regularity of primary and secondary muscle spindle afferent discharges. *J Physiol.* 1969; 202:59–82. [PubMed: 4238988]
- McConville KM, Tomlinson RD. Behavior of eye-movement-related cells in the vestibular nuclei during combined rotational and translational stimuli. *J Neurophysiol.* 1996; 76:3136–3148. [PubMed: 8930261]
- McCrea RA, Chen-Huang C, Belton TM, Gdowski GT. Behavior contingent processing of vestibular sensory signals in the vestibular nuclei. *Ann NY Acad Sci.* 1996; 781:292–303. [PubMed: 8694421]
- McCrea RA, Gdowski GT, Boyle R, Belton T. Firing behavior of vestibular neurons during active and passive head movements: vestibulospinal and other non-eye-movement related neurons. *J Neurophysiol.* 1999; 82:416–428. [PubMed: 10400968]
- McCue MP, Guinan JJ Jr. Influence of efferent stimulation on acoustically responsive vestibular afferents in the cat. *J Neurosci.* 1994; 14:6071–6083. [PubMed: 7931563]
- McFarland JL, Fuchs AF. Discharge patterns in nucleus prepositus hypoglossi and adjacent medial vestibular nucleus during horizontal eye movement in behaving macaques. *J Neurophysiol.* 1992; 68:319–332. [PubMed: 1517825]
- Mensing AF, Carey JP, Boyle R, Highstein SM. Differential central projections of physiologically characterized horizontal semicircular canal vestibular nerve afferents in the toad-fish, *Opsanus tau*. *J Comp Neurol.* 1997; 384:71–85. [PubMed: 9214541]

- Merigan WH, Maunsell JH. How parallel are the primate visual pathways? *Annu Rev Neurosci.* 1993; 16:369–402. [PubMed: 8460898]
- Minor LB, Goldberg JM. Vestibular-nerve inputs to the vestibulo-ocular reflex: a functional-ablation study in the squirrel monkey. *J Neurosci.* 1991; 11:1636–1648. [PubMed: 2045879]
- Minor LB, McCrea RA, Goldberg JM. Dual projections of secondary vestibular axons in the medial longitudinal fasciculus to extraocular motor nuclei and the spinal cord of the squirrel monkey. *Exp Brain Res.* 1990; 83:9–21. [PubMed: 2073953]
- Mountcastle, VB. Central nervous mechanisms in mechanoreceptive sensibility. In: Darian-Smith, I., editor. *Handbook of physiology. Section I. The nervous system. Volume III. Sensory processes, part 2.* Williams & Wilkins; Baltimore: 1984. p. 789-878.
- Myers SF, Lewis ER. Hair cell tufts and afferent innervation of the bullfrog crista ampullaris. *Brain Res.* 1990; 534:15–24. [PubMed: 1705850]
- Newlands SD, Perachio AA. Compensation of horizontal canal related activity in the medial vestibular nucleus following unilateral labyrinth ablation in the decerebrate gerbil. I. Type I neurons. *Exp Brain Res.* 1990; 82:359–372. [PubMed: 2286238]
- Oertel D. The role of intrinsic neuronal properties in the encoding of auditory information in the cochlear nuclei. *Curr Opin Neurobiol.* 1991; 1:221–228. [PubMed: 1821185]
- Paige GD. Vestibuloocular reflex and its interactions with visual following mechanisms in the squirrel monkey. I. Response characteristics in normal animals. *J Neurophysiol.* 1983; 49:134–151. [PubMed: 6827291]
- Palmer AR. Physiology of the cochlear nerve and cochlear nucleus. *Br Med Bull.* 1987; 43:838–855. [PubMed: 3329928]
- Peterson BW, Baker JF, Perlmutter SI, Iwamoto Y. Neuronal substrates of spatial transformations in vestibuloocular and vestibulocollic reflexes. *Ann NY Acad Sci.* 1992; 656:485–499. [PubMed: 1599164]
- Peterson EH. Are there parallel channels in the vestibular nerve? *News Physiol Sci.* 1998; 13:194–201. [PubMed: 11390788]
- Peusner KD, Giaume C. The first developing “mixed” synapses between vestibular sensory neurons mediate glutamate chemical transmission. *Neuroscience.* 1994; 58:99–113. [PubMed: 7909147]
- Pulaski PD, Zee DS, Robinson DA. The behavior of the vestibulo-ocular reflex at high velocities of head rotation. *Brain Res.* 1981; 222:159–165. [PubMed: 7296263]
- Raphan T, Matsuo V, Cohen B. Velocity-storage in the vestibulo-ocular reflex arc (vor). *Exp Brain Res.* 1979; 35:229–248. [PubMed: 108122]
- Rapoport S, Susswein A, Uchino Y, Wilson VJ. Properties of vestibular neurones projecting to neck segments of the cat spinal cord. *J Physiol.* 1977a; 268:493–510. [PubMed: 874918]
- Rapoport S, Susswein A, Uchino Y, Wilson VJ. Synaptic actions of individual vestibular neurones on cat neck-motoneurones. *J Physiol.* 1977b; 272:367–382. [PubMed: 592195]
- Raymond J, Dechesne CJ, Desmadryl G, Demêmes D. Different calcium-binding proteins identify subpopulations of vestibular ganglion neurons in the rat. *Acta Otolaryngol Suppl.* 1993; 503:114–118. [PubMed: 8385864]
- Rennie KJ, Correia MJ. Potassium currents in mammalian and avian isolated type I semicircular canal hair cells. *J Neurophysiol.* 1994; 71:317–329. [PubMed: 8158233]
- Rice SO. Mathematical analysis of random noise. *Bell Sys Tech J.* 1944; 23:282–332.
- Robinson, DA. Vestibular and optokinetic symbiosis: an example of explaining by modelling. In: Baker, R.; Berthoz, A., editors. *Control of gaze by brain stem neurons.* Elsevier; Amsterdam: 1977. p. 49-58.
- Rossi ML, Martini M, Pelucchi B, Fesce R. Quantal nature of synaptic transmission at the cytoneural junction in the frog labyrinth. *J Physiol.* 1994; 478:17–35. [PubMed: 7965832]
- Roy JE, Cullen KE. A neural correlate for vestibuloocular reflex suppression during voluntary eye-head gaze shifts. *Nature Neuroscience.* 1998; 1:404–410.
- Rüsch A, Eatock RA. Voltage responses of mouse utricular hair cells to injected current. *Ann NY Acad Sci.* 1996a; 781:71–84. [PubMed: 8694485]

- Rüsch A, Eatock RA. A delayed rectifier conductance in type I hair cells of the mouse utricle. *J Neurophysiol.* 1996b; 76:995–1004. [PubMed: 8871214]
- Sato F, Sasaki H. Morphological correlations between spontaneously discharging primary vestibular afferents and vestibular nucleus neurons in the cat. *J Comp Neurol.* 1993; 333:554–566. [PubMed: 8370817]
- Sato F, Sasaki H, Ishizuka N, Sasaki S, Mannen H. Morphology of single primary vestibular afferents originating from the horizontal semicircular canal in the cat. *J Comp Neurol.* 1989; 290:423–439. [PubMed: 2592621]
- Sato H, Endo K, Ikegami H, Imagawa M, Sasaki M, Uchino Y. Properties of utricular nerve-activated vestibulospinal neurons in cats. *Exp Brain Res.* 1996; 112:197–202. [PubMed: 8951388]
- Sato H, Imagawa M, Isu N, Uchino Y. Properties of saccular nerve-activated vestibulospinal neurons in cats. *Exp Brain Res.* 1997; 116:381–388. [PubMed: 9372287]
- Schiller PH, Logothetis NK. The color-opponent and broad-band channels of the primate visual system. *Trends Neurosci.* 1990; 13:392–398. [PubMed: 1700509]
- Schneider LW, Anderson DJ. Transfer characteristics of first and second order lateral canal vestibular neurons in gerbil. *Brain Res.* 1976; 112:61–76. [PubMed: 947494]
- Scudder CA, Fuchs AF. Physiological and behavioral identification of vestibular nucleus neurons mediating the horizontal vestibuloocular reflex in trained rhesus monkeys. *J Neurophysiol.* 1992; 68:244–264. [PubMed: 1517823]
- Serafin M, Waele C de, Khateb A, Vidal PP, Muhlethaler M. Medial vestibular nucleus in the guinea-pig. I. Intrinsic membrane properties in brainstem slices. *Exp Brain Res.* 1991a; 84:417–425. [PubMed: 2065749]
- Serafin M, Waele C de, Khateb A, Vidal PP, Muhlethaler M. Medial vestibular nucleus in the guinea-pig. II. Ionic basis of the intrinsic membrane properties in brainstem slices. *Exp Brain Res.* 1991b; 84:426–433. [PubMed: 1648506]
- Shannon CE. A mathematical theory of communication. *Bell Sys Tech J.* 1948; 17:379–424. 623–657.
- Shannon CE. Communication in the presence of noise. *Proc Inst Radio Eng.* 1949; 37:10–21.
- Shapley R. Visual sensitivity and parallel retinocortical channels. *Annu Rev Psychol.* 1990; 41:635–658. [PubMed: 2407178]
- Smith PF, Curthoys IS. Mechanisms of recovery following unilateral labyrinthectomy: a review. *Brain Res Brain Res Rev.* 1989; 14:155–180. [PubMed: 2665890]
- Smith CE, Goldberg JM. A stochastic afterhyperpolarization model of repetitive activity in vestibular afferents. *Biol Cybern.* 1986; 54:41–51. [PubMed: 3487348]
- Stein RB. The information capacity of nerve cells using a frequency code. *Biophys J.* 1967; 7:797–826. [PubMed: 19210999]
- Stein, RB. The role of spike trains in transmitting and distorting sensory signals. In: Schmitt, FO., editor. *The neurosciences – second study program.* Rockefeller University Press; New York: 1970. p. 597–604.
- Stein RB, French AS, Holden AV. The frequency response, coherence, and information capacity of two neuronal models. *Biophys J.* 1972; 12:295–322. [PubMed: 5016114]
- Straka H, Dieringer N. Uncrossed disynaptic inhibition of second-order vestibular neurons and its interaction with mono-synaptic excitation from vestibular nerve afferent fibers in the frog. *J Neurophysiol.* 1996; 76:3087–3101. [PubMed: 8930257]
- Straka H, Biesdorf S, Dieringer N. Canal-specific excitation and inhibition of frog second-order vestibular neurons. *J Neurophysiol.* 1997; 78:1363–1372. [PubMed: 9310427]
- Sugai T, Sugitani M, Ooyama H. Effects of activation of the divergent efferent fibers on the spontaneous activity of vestibular afferent fibers in the toad. *Jpn J Physiol.* 1991; 41:217–232. [PubMed: 1942662]
- Takahashi Y, Tsumoto T, Kubo T. N-methyl-D-aspartate receptors contribute to afferent synaptic transmission in the me-dial vestibular nucleus of young rats. *Brain Res.* 1994; 659:287–291. [PubMed: 7820677]
- Tomlinson RD, Robinson DA. Signals in vestibular nucleus mediating vertical eye movements in the monkey. *J Neurophysiol.* 1984; 51:1121–1136. [PubMed: 6737024]

- Troy JB, Lee BB. Steady discharges of macaque retinal ganglion cells. *Vis Neurosci.* 1994; 11:111–118. [PubMed: 8011574]
- Troy JB, Robson JG. Steady discharges of X and Y retinal ganglion cells of cat under photopic illuminance. *Vis Neurosci.* 1992; 9:535–553. [PubMed: 1450106]
- Trussell LO. Cellular mechanisms for preservation of timing in central auditory pathways. *Curr Opin Neurobiol.* 1997; 7:487–492. [PubMed: 9287194]
- Trussell LO. Synaptic mechanisms for coding timing in auditory neurons. *Annu Rev Physiol.* 1999; 61:477–496. [PubMed: 10099698]
- Uchino Y, Sasaki M, Sato H, Imagawa M, Suwa H, Isu N. Utriculoocular reflex arc of the cat. *J Neurophysiol.* 1996; 76:1896–1903. [PubMed: 8890302]
- Verveen AA, DeFelice LJ. Membrane noise. *Prog Biophys Mol Biol.* 1974; 28:189–265. [PubMed: 4617247]
- Vidal PP, Babalian A, Vibert N, Serafin M, Muhlethaler M. In vivo – in vitro correlations in the central vestibular system: a bridge too far? *Ann NY Acad Sci.* 1996; 781:424–436. [PubMed: 8694432]
- Viirre E, Tweed D, Milner K, Vilis T. A reexamination of the gain of the vestibuloocular reflex. *J Neurophysiol.* 1986; 56:439–450. [PubMed: 3489820]
- Wersäll, J.; Bagger-Sjöbäck, D. Morphology of the vestibular sense organ. In: Kornhuber, HH., editor. *Handbook of sensory physiology, vol VI. Vestibular system. Part 1. Basic mechanisms.* Springer; Berlin Heidelberg New York: 1974. p. 123-170.
- Wilson VJ, Maeda M. Connections between semicircular canals and neck motoneurons in the cat. *J Neurophysiol.* 1974; 37:346–357. [PubMed: 4815209]
- Wilson VJ, Wylie RM. A short-latency labyrinthine input to the vestibular nuclei in the pigeon. *Science.* 1970; 168:124–127. [PubMed: 5417052]
- Wilson VJ, Peterson BW, Fukushima K, Hirai N, Uchino Y. Analysis of vestibulocollic reflexes by sinusoidal polarization of vestibular afferent fibers. *J Neurophysiol.* 1979; 42:331–346. [PubMed: 311377]
- Wylie RM. Evidence of electrotonic transmission in the vestibular nuclei of the rat. *Brain Res.* 1973; 50:179–83. [PubMed: 4347844]
- Yagi T, Simpson NE, Markham CH. The relationship of conduction velocity to other physiological properties of the cat's horizontal canal neurons. *Exp Brain Res.* 1977; 30:587–600. [PubMed: 598443]
- Young ED, Spirou GA, Rice JJ, Voigt HF. Neural organization and responses to complex stimuli in the dorsal cochlear nucleus. *Philos Trans R Soc Lond B.* 1992; 336:407–413. [PubMed: 1354382]

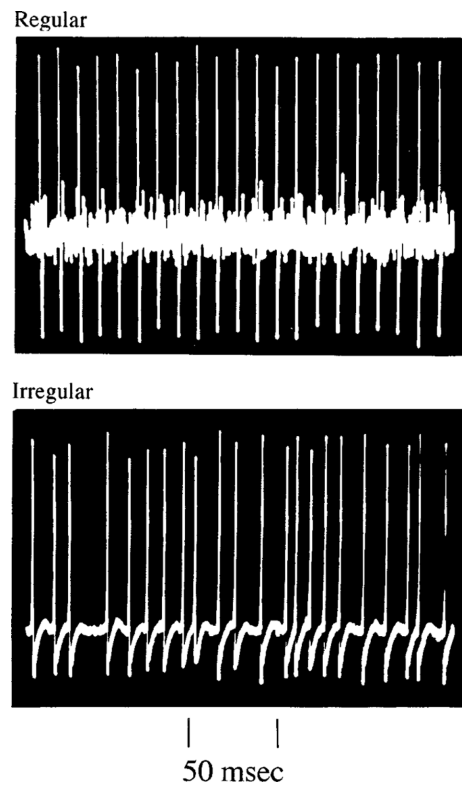


Fig. 1. Discharge regularity in vestibular-nerve afferents. Spike trains from two afferents, each innervating the superior crista in a squirrel monkey. Both fibers are firing at nearly the same rate, slightly less than 100 spikes/s. The top unit has a regular discharge, the bottom unit an irregular discharge. From Goldberg and Fernández (1971a)

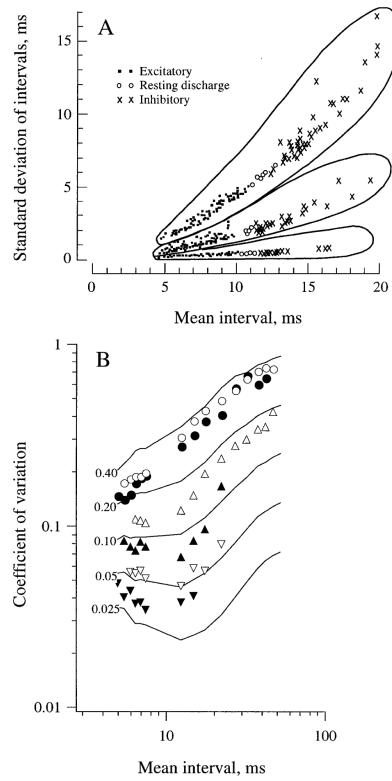


Fig. 2A, B.

Discharge regularity is characteristic of each afferent. **A** Standard deviation of intervals versus mean interval for three semicircular-canal afferents in the squirrel monkey. From Goldberg and Fernández (1971b). **B** Relation between coefficient of variation (cv) and mean interval (\bar{t}) for six semicircular-canal afferents in the squirrel monkey, indicated by different symbols. The points for individual units conform to the empirical curves relating cv and \bar{t} for different values of cv^* , the cv at \bar{t} ms (see *numbers to the left*). Based on Goldberg et al. (1984)

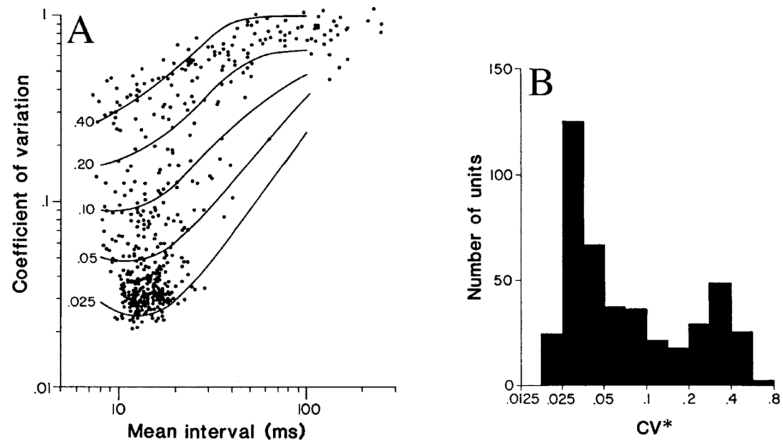


Fig. 3A, B.

Quantifying discharge regularity. **A** The curves are empirical functions, based on the relation between the coefficient of variation (cv) and the mean interval $\bar{\tau}$ for individual chinchilla otolith afferents, whose discharge rates were changed by static tilts. Each curve is for a particular normalized cv^* , the cv at $\bar{\tau}=15$ ms (see *numbers to left*). Each point shows cv versus $\bar{\tau}$ at the resting discharge for an individual chinchilla semicircular-canal unit. **B** cv^* 's for a population of chinchilla semicircular-canal units. From Baird et al. (1988)

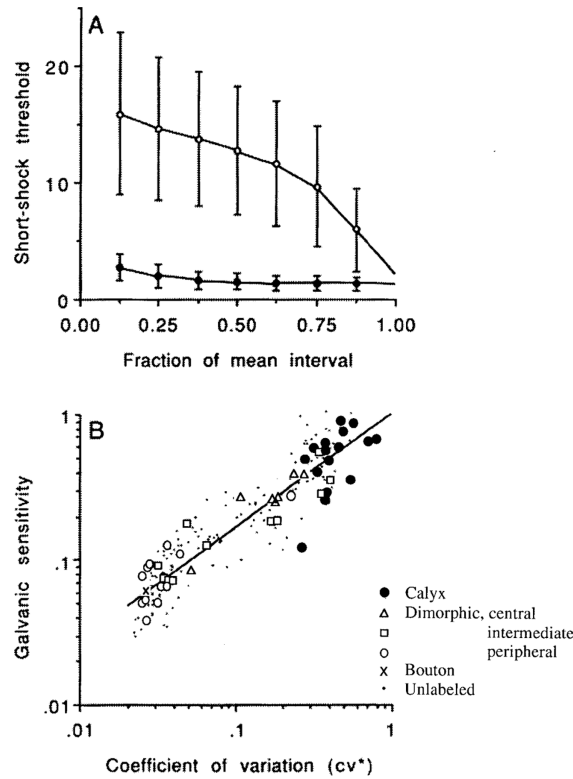


Fig. 4A, B.

Responses of vestibular-nerve afferents to electrical stimulation delivered by an electrode in the perilymphatic space of the vestibule. **A** Thresholds for 0.1-ms shocks presented at stated times after the occurrence of a naturally occurring action potential at $t=0$. Squirrel-monkey afferents. Time is expressed as a fraction (f) of the mean interval; threshold is normalized in each animal to a value of unity at $f=1$ in the most sensitive afferents. *Points* are means and *bars* are standard deviations for populations of regular (\circ) and irregular (\odot) afferents. Recovery in irregular units is fast; that in regular units is delayed. From Goldberg et al. (1990c), based on Goldberg et al. (1984). **B** Sensitivity determined from the response to the last 2.5 s of a 5-s, 50- μ A current is plotted against the normalized coefficient of variation (cv^*) for chinchilla semicircular-canal afferents. For each animal, sensitivity is normalized to unity for $cv^*=1$ by an analysis of covariance that estimates sensitivity differences across preparations; such differences are likely to reflect electrode placement or other technical factors. *Key*, symbols representing labeled and unlabeled fibers; *straight-line*, best fitting power-law relation. The more irregular the afferent, the more sensitive it is to galvanic currents. From Goldberg et al. (1990c), based on Baird et al. (1988)

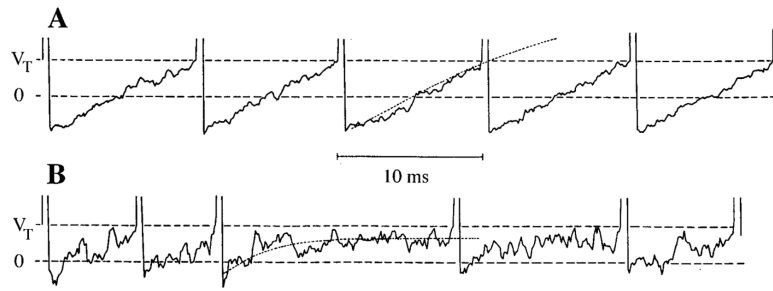


Fig. 5A, B.

A stochastic version of an afterhyperpolarization (AHP) model of repetitive discharge. 0 Resting potential, V_T spike-threshold potential. Two model units are shown with their mean interspike trajectories (*dotted lines*). **A** The unit at the top has a regular discharge because of its deep and slow AHP and relatively small miniature EPSPs. **B** The bottom unit is irregular as its AHP is shallow and fast and its miniature EPSPs somewhat larger than those in **A**. Note that a regular discharge is associated with the mean trajectory crossing V_T . For the irregular discharge, the mean trajectory does not cross V_T . As a result, the timing of spikes in the regular unit is largely determined by the mean trajectory, whereas that for the irregular unit is largely determined by synaptic noise. From Smith and Goldberg (1986)

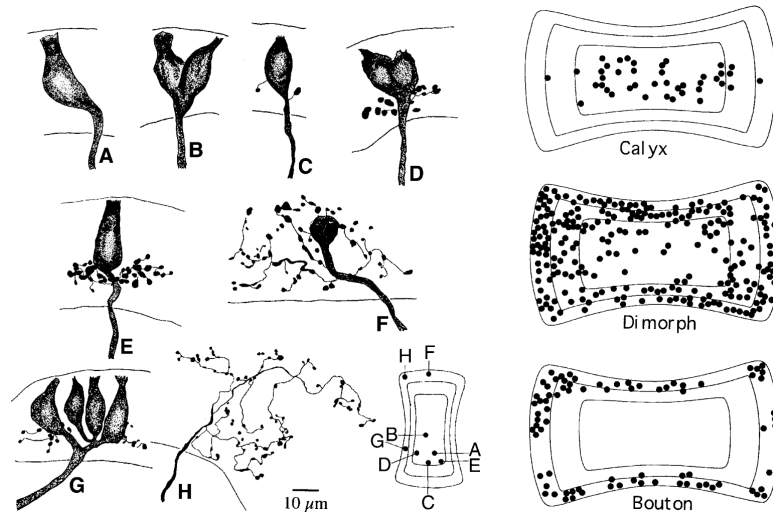


Fig. 6A–H.

Innervation patterns in the chinchilla crista, as revealed by extracellular horseradish-peroxidase (HRP) labeling of individual afferents. **A, B** Calyx fibers innervating one or two hair cells. **C–G** Dimorphic fibers include both calyx and bouton endings. **H** Bouton fiber. *Inset* Locations of individual afferents are placed on a standard map of the crista. *Right* Three standard maps of the crista divided into concentrically arranged central, intermediate, and peripheral zones of equal areas. Shown are the locations of calyx, dimorphic, and bouton fibers with each symbol (●) representing a single dye-filled fiber. Dimorphic units make up 70% of the population, bouton units 20%, and calyx units 10%. From Fernández et al. (1988)

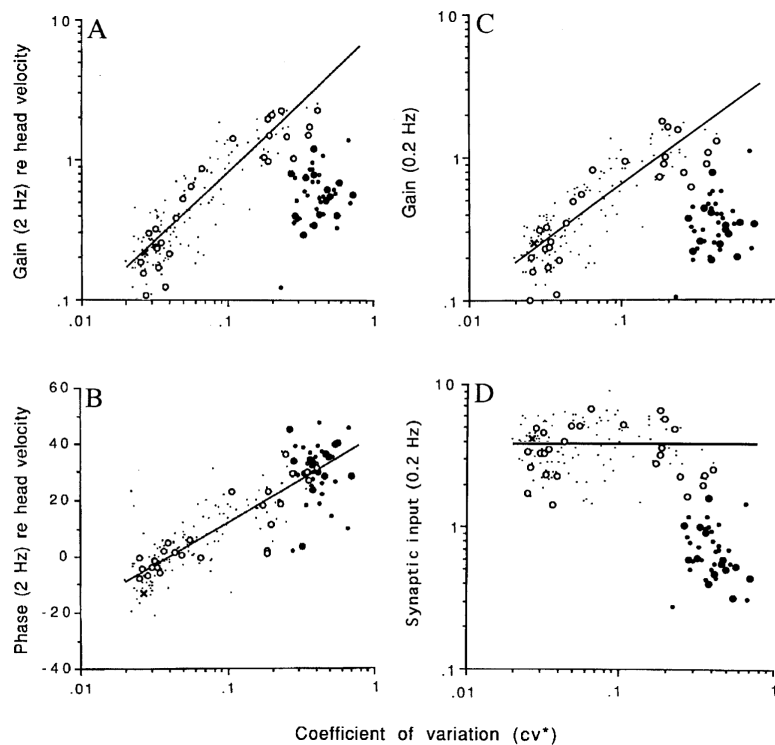


Fig. 7A–D.

Responses of semicircular-canal afferents in the chinchilla to sinusoidal head rotations. Each *point* represents an individual unit. Labeled afferents include calyx (●), dimorphic (○), and bouton (×) fibers; *smaller dots* represent unlabeled fibers. **A** Rotational gain re head velocity (spikes·s⁻¹/°s⁻¹) versus normalized coefficient of variation (cv^*). *Straight-line*, best fitting power-law relation between gain and cv^* for dimorphic and bouton fibers. Data are for 2-Hz sinusoidal rotations. **B** Rotational phase re head velocity (degrees) for the same sinusoidal head rotations versus cv^* . *Straight-line*, best fitting semilogarithmic relation between phase and cv^* for all fibers. When compared with irregular dimorphic units with similar cv^* s, calyx units have considerably lower gains, but similar phases. **C** Based on an empirical transfer function, gains at 0.2 Hz have been calculated from the 2-Hz gains in **A**. The power-law relation for dimorphic and bouton units in **C** is less steep than the relation in **A** and is virtually identical with the power-law relation between normalized galvanic sensitivity (β^*) and cv^* (Fig. 4B). **D** As a result of the similarity in power-law relations, synaptic input, the ratio between the rotational gain of each unit at 0.2 Hz and normalized galvanic sensitivity, is nearly constant for dimorphic and bouton units regardless of their discharge regularity. Calyx units are distinctive in having a much lower synaptic input than other units. From Goldberg et al. (1990c), based on Baird et al. (1988)

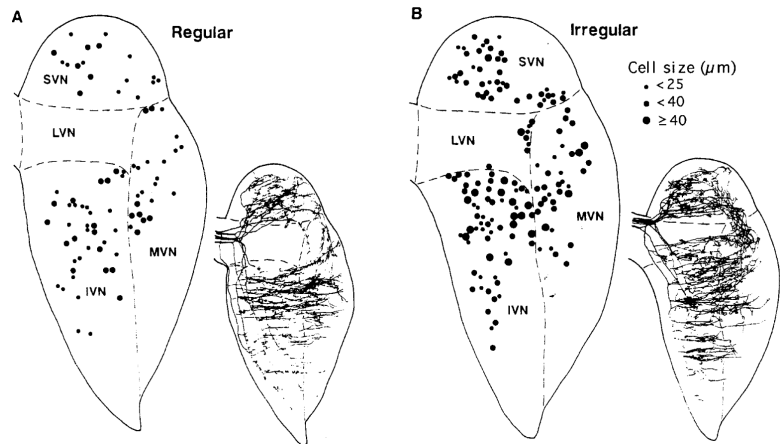


Fig. 8A, B.

Innervation by HRP-labeled horizontal-canal afferents of the vestibular nuclei of the cat. Standard horizontal sections of the four main nuclei: superior (*SVN*), lateral (*LVN*), inferior or descending (*IVN*), and medial (*MVN*) vestibular nuclei. Afferents were characterized as regular (**A**) or irregular (**B**). In each *subpanel*, the *drawing to the left* indicates size of cell bodies receiving boutons (*key to right*), whereas the smaller *drawing to the right* depicts branching patterns for several afferents. From Sato and Sasaki (1993)

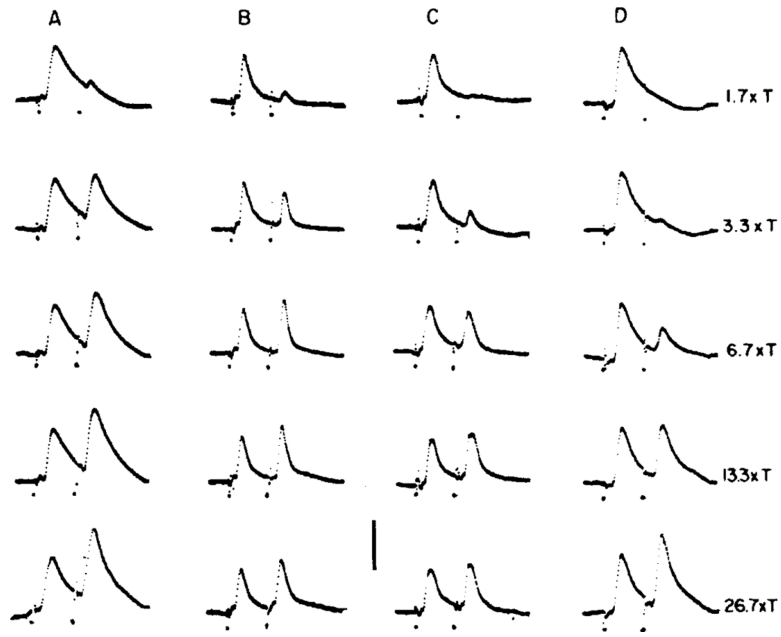


Fig. 9A–D.

An intracellular paradigm can deduce the profile of regular and irregular inputs received by individual secondary neurons. EPSPs were recorded from four cells (**A–D**) located in the superior vestibular nucleus of one squirrel monkey. Each record includes the response to a supramaximal shock intended to synchronize the activity of the vestibular nerve. This is followed 4 ms later by a second shock ranging in amplitude from 1.7 to 26.7xT, where T is the threshold shock strength needed to evoke a field potential in the vestibular nuclei. **A** This cell receives a predominantly irregular vestibular-nerve input because the second EPSP reaches near-maximal size at low shock strengths. **D** In this case, the vestibular-nerve input is predominantly regular, as the second EPSP is activated only at high shock strengths. **B, C** These two cells receive mixed irregular and regular inputs. The second EPSP has a low threshold, but continues to grow as shock strength increases. Calibration: 10 mV (**A, B**) and 5 mV (**C, D**). From Goldberg et al. (1987)

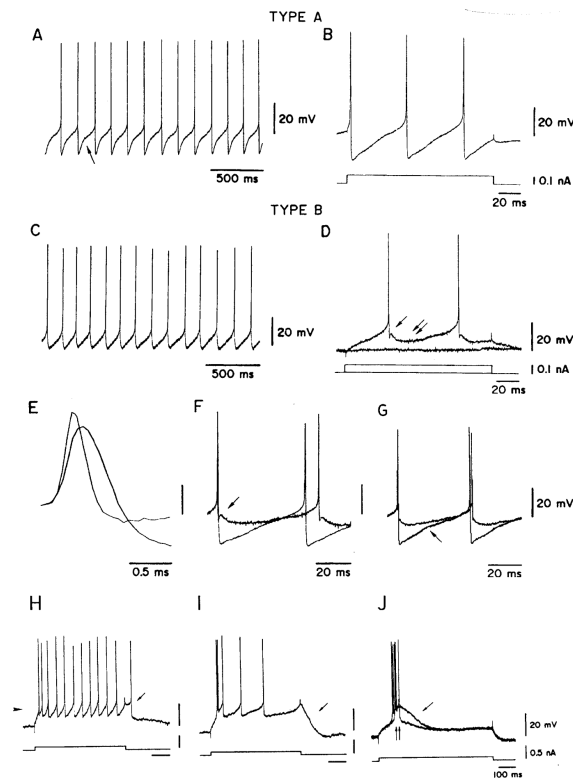


Fig. 10A–J.

Properties of “A” and “B” neurons recorded from slices through the medial vestibular nucleus in the guinea pig. **A** Spontaneous activity in an “A” neuron. The slowing of the afterhyperpolarization (AHP) trajectory (see *arrow*) suggests the presence of an A-like current. **B** The same “A” neuron is seen responding to depolarizing currents at a higher speed to show the single AHP following each spike. **C** Spontaneous activity in a “B” neuron. **D** Response of the “B” neuron to depolarizing currents is seen at higher speed. The AHP shows a fast component (*arrow*), followed by a slow component (*double arrow*). No additional slowing of the AHP is seen as the neuron depolarizes towards firing threshold. **E** Spikes recorded in “A” and “B” neurons. Action potentials are wider in “A” neurons. **F, G** AHPs are superimposed for an “A” neuron (**G**, *lower arrow*) and a “B” neuron (**F**, *upper arrow*). These potentials are larger in “A” neurons. **H–J** Response to depolarizing currents of a “B” neuron. Tonic firing in **H** is replaced by plateau potentials (**I–J**, *single arrows*) and by low-threshold Ca^{2+} spikes (**J**, *double arrows*) as the cell is depolarized from progressively more hyperpolarized levels. From Serafin et al. (1991a)

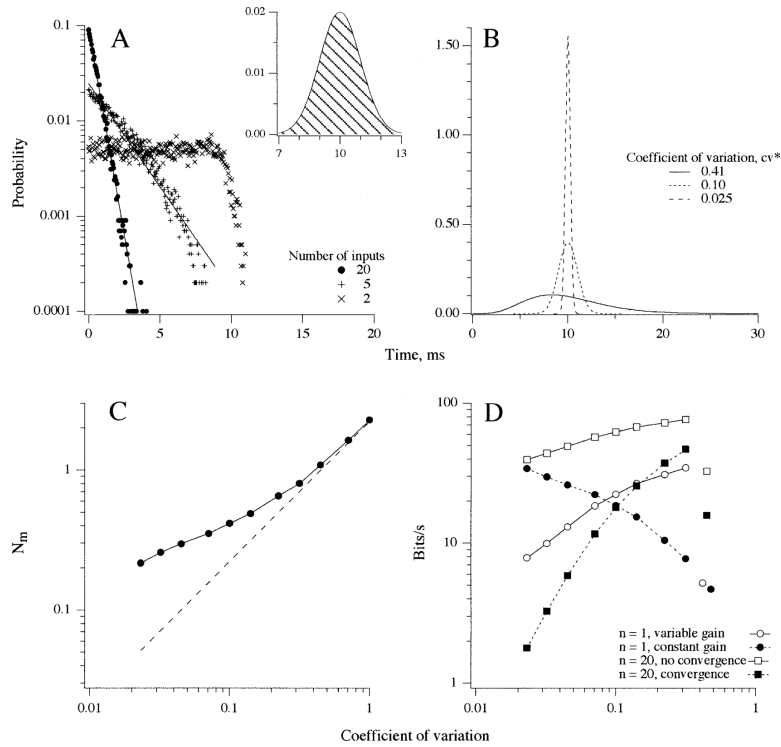


Fig. 11A–D.

Theoretical considerations in information transmission between vestibular-nerve afferents and secondary neurons. **A** Simulated interval distributions obtained by the superposition of several unsynchronized afferents (see *key*), each having an intermediate regularity (see *inset*). Even two inputs result in an irregular discharge. The interval distribution approaches an exponential distribution, appropriate to a Poisson process, when the number of inputs reaches five. **B** Eq. 2 was used to calculate interval distributions with mean intervals of 10 ms and varying coefficients of variation (*cv*) (see *key*). **C** Simulations were used to determine $\bar{N}_m(\Delta T)$, the standard deviation in the number of events as a function of the coefficient of variation for a single input. Actual values of $\bar{N}_m(\Delta T)$ (*solid line*) are compared with the linear approximation, $\bar{N}_m(\Delta T) = (\Delta t / \mu)^{1/2}$ (*dashed line*), which holds for long sampling intervals (Cox 1962). In the particular case considered, the sampling interval, $\Delta t = 50$ ms, and the mean interval, $\Delta = 10$ ms. For each *cv*, the appropriate gamma distribution was chosen and its equilibrium and waiting-time distributions used in a Monte-Carlo simulation of the events occurring in 100 separate, 50-ms samples. The number of events in the several samples was used to calculate $\bar{N}_m(\Delta T)$. **D** $I(\Delta t)$, the information transmitted in bits/s during $\Delta t = 50$ ms is calculated from eq. 1, with $\bar{N}_m(\Delta T)$ obtained from **C**. Curves are for theoretical dimorphic (and bouton) units, whose *cv*'s vary from 0.0231 to 0.316. *Points to the right* are for a theoretical calyx unit with a *cv* = 0.447. Calculations were done for single afferents ($n=1$) and for $n=20$ afferents kept separate or converging on a single secondary neuron. For $n=1$, constant gain, $S_m(\Delta t) = 0.674$. For all other curves, $S_m(\Delta t) = k \cdot cv$ is assumed to be linearly related to *cv*. The proportionality constant, $k = 8$ spikes, was set so that the highest value is $S_m(\Delta t) = 2.5$ spikes at *cv* = 0.316, compared with a background of $\lambda \Delta t = 5$ spikes. This value of S_m minimizes inhibitory silencing for even the most sensitive unit. Afferent gains, g , for dimorphic units are linearly related to *cv* with a proportionality constant, $k = 8$ spikes \cdot s $^{-1}$ / degrees s $^{-1}$ (Fig. 7A). The rms stimulus amplitude corresponding to $k = 8$ spikes is $S_x = k / k_f \Delta t = 20$ degrees/s. From human data (Grossman et al. 1988), this value of S_x matches head velocities during walking, is slightly smaller than those during

running, and considerably smaller than those during maximal voluntary head shakes. *Single points to the right* are for the calyx unit with $S_m(\Delta t)=0.72$, five times smaller than predicted from the linear relation between $S_m(\Delta t)$ and cv for dimorphic units

Table 1

Characteristics of regularly and irregularly discharging afferents, mammalian vestibular nerve

Irregularly discharging	Regularly discharging
^a Thick and medium-sized axons ending as calyx and dimorphic terminals in the central (striolar) zone	Medium-sized and thin axons ending as dimorphic and bouton terminals in the peripheral (peripheral extrastriolar) zone
^b Phasic-tonic response dynamics, including a sensitivity to the velocity of cupular (otolith) displacement	Tonic response dynamics, resembling those expected of end-organ macromechanics
^b High sensitivity to angular or linear forces acting on the head (Calyx units innervating the cristae have an irregular discharge and low sensitivities)	Low sensitivity to angular or linear forces
^c Large responses to electrical stimulation of efferent fibers	Small responses to electrical stimulation of efferent fibers
^d Low thresholds to short shocks and large responses to constant galvanic currents, both delivered via the perilymphatic space	High thresholds and small responses to the same galvanic stimuli

^aGoldberg and Fernández 1977; Yagi et al. 1977; Baird et al. 1988; Goldberg et al. 1990a; Lysakowski et al. 1995

^bGoldberg and Fernández 1971b; Yagi et al. 1977; Fernández and Goldberg 1976b; Baird et al. 1988; Goldberg et al. 1990a; Lysakowski et al. 1995

^cGoldberg and Fernández 1980; McCue and Guinan 1994

^dEzure et al. 1983; Goldberg et al. 1982, 1984, 1987; Brontë-Stewart and Lisberger 1994

Table 2Discharge regularity, different sensory axons. Rate in spikes/s. *cv* Coefficient of variation

System	Organ or type	Rate	cv
Vestibular, mammals ^a	Semicircular canals, squirrel monkey	50–100	0.025–0.6
	Otolith organs, squirrel monkey	50–100	0.025–0.6
Retinal, cat ^b	X-on center	53 (35)	0.38 (0.48)
	X-off center	18 (35)	0.54 (0.42)
	Y-on center	29 (35)	0.61 (0.59)
	Y-off center	5 (35)	0.68 (0.51)
Cochlear, cat ^c	Type I, all spontaneous groups	15	0.82
Muscle spindle, cat ^d	Primary receptors, de-efferented	25–33	0.063
	Secondary receptors, de-efferented	25–33	0.020
	Primary receptors, with efferents	25–33	0.25
	Secondary receptors, with efferents	25–33	0.063
Slowly adapting cutaneous mechanoreceptors ^e	SA I	17.5	0.63
	SA II	16.6	0.05

^aGoldberg et al. 1984; Baird et al. 1988

^bTroy and Robson 1992; Troy and Lee 1994. Two sets of *cv*'s are given. Those *outside of parentheses* refer to the typical rates, also *outside of parentheses*. Those *inside parentheses* are for a fixed rate of 35 spikes/s

^cLi and Young 1993; E. D. Young, personal communication

^dMatthews and Stein 1969. To normalize the *cv*'s, the authors chose a narrow range of discharge rates

^eIggo and Muir 1969